Molecular Cell
Article

Commitment to a Cellular Transition Precedes Genome-wide Transcriptional Change

Umut Eser,[1,2] Melody Falleur-Fettig,[2] Amy Johnson,[2] and Jan M. Skotheim[2,*]
[1]Department of Applied Physics
[2]Department of Biology
Stanford University, Stanford CA 94305, USA
*Correspondence: skotheim@stanford.edu
DOI 10.1016/j.molcel.2011.06.024

SUMMARY

In budding yeast, commitment to cell division corresponds to activating the positive feedback loop of G1 cyclins controlled by the transcription factors SBF and MBF. This pair of transcription factors has over 200 targets, implying that cell-cycle commitment coincides with genome-wide changes in transcription. Here, we find that genes within this regulon have a well-defined distribution of transcriptional activation times. Combinatorial use of SBF and MBF results in a logical OR function for gene expression and partially explains activation timing. Activation of G1 cyclin expression precedes the activation of the bulk of the G1/S regulon, ensuring that commitment to cell division occurs before large-scale changes in transcription. Furthermore, we find similar positive feedback-first regulation in the yeasts *S. bayanus* and *S. cerevisiae*, as well as human cells. The widespread use of the feedback-first motif in eukaryotic cell-cycle control, implemented by nonorthologous proteins, suggests its frequent deployment at cellular transitions.

INTRODUCTION

Order may be produced in a sequence of biochemical events through feedback control mechanisms or substrate-specific chemical kinetics. In the cell cycle, regulatory checkpoints ensure the proper order of many essential events through feedback control. DNA replication must be finished and damage repaired before mitosis, while anaphase is initiated only after complete spindle assembly (Morgan 2007). Checkpoints use designated regulatory molecules to restrain cell-cycle progression until a set of criteria are satisfied (Hartwell and Weinert 1989). However, order without checkpoint control is observed in *Xenopus* embryos as cell-cycle events are entrained by oscillations in cyclin dependent kinase (CDK) activity. Furthermore, addition of CDK substrates to *Xenopus* egg extracts in different stages of mitosis revealed that the order of substrate phosphorylation is independent of cell-cycle phase (Georgi et al., 2002). Thus, temporal order of phosphorylation in mitosis is likely the result of substrate-specific kinetics. Here, we investigate the integration of chemical kinetics and feedback control at the *Start* transition in budding yeast.

Start marks the point of commitment to the mitotic cell cycle, which is located between cell division and DNA replication (Hartwell et al., 1974). Prior to *Start*, cells integrate internal (e.g., cell size) and external (e.g., mating pheromone) signals to make an all-or-none decision to divide. Beyond *Start*, cells are committed to divide regardless of changes in extracellular signals. In another article in this issue, we show that passage through *Start* corresponds precisely to the activation of the G1 cyclin-positive feedback loop (Dončić et al., 2011). Thus, *Start* is a member of a growing list of cellular and developmental transitions driven by positive feedback (Pomerening et al., 2003; Xiong and Ferrell 2003; Holt et al., 2008; Justman et al., 2009; López-Avilés et al., 2009).

Positive feedback at *Start* is initiated by the G1 cyclin, Cln3 in complex with the cyclin dependent kinase Cdc28 (Figure 1A). The primary target of Cln3 is the transcriptional inhibitor Whi5, whose inactivation is rate limiting for the expression of the G1/S regulon (Costanzo et al., 2004; de Bruin et al., 2004). Cln3-Cdc28 phosphorylates and initiates Whi5 inactivation, which allows some transcription of two additional G1 cyclins, *CLN1* and *CLN2* (Tyers et al., 1993). The downstream G1 cyclins then complete the positive feedback loop through the inactivation and nuclear exclusion of Whi5 and the full activation of the transcription factors SBF (Swi4-Swi6) and MBF (Mbp1-Swi6) (Andrews and Herskowitz 1989; Nasmyth and Dirick 1991; Koch et al., 1993; de Bruin et al., 2004; Skotheim et al., 2008).

Surprisingly, the transcription factors at the center of the positive feedback loop, SBF and MBF, are also responsible for the transcription of over 200 additional genes (Ferrezuelo et al., 2010). Indeed, cell-cycle commitment appears to coincide with the coordinated transcriptional activation of approximately 5% of all genes (Spellman et al., 1998). Although Whi5 phosphorylation is rate limiting for activation of positive feedback, it is also likely to be rate limiting for the transcription of all SBF regulated genes due to the direct Whi5-SBF interaction (de Bruin et al., 2004). The concurrent activation of the related heterodimeric transcription factor MBF also requires CDK activity, possibly through phosphorylation of the shared component Swi6 (Wijnen et al., 2002). Thus, given the integrated nature of the regulatory circuit and the ability of the upstream cyclin Cln3 to activate SBF- and MBF-dependent transcription in *cln1Δ cln2Δ* cells (Dirick et al., 1995; Stuart and Wittenberg 1995), it is unclear if

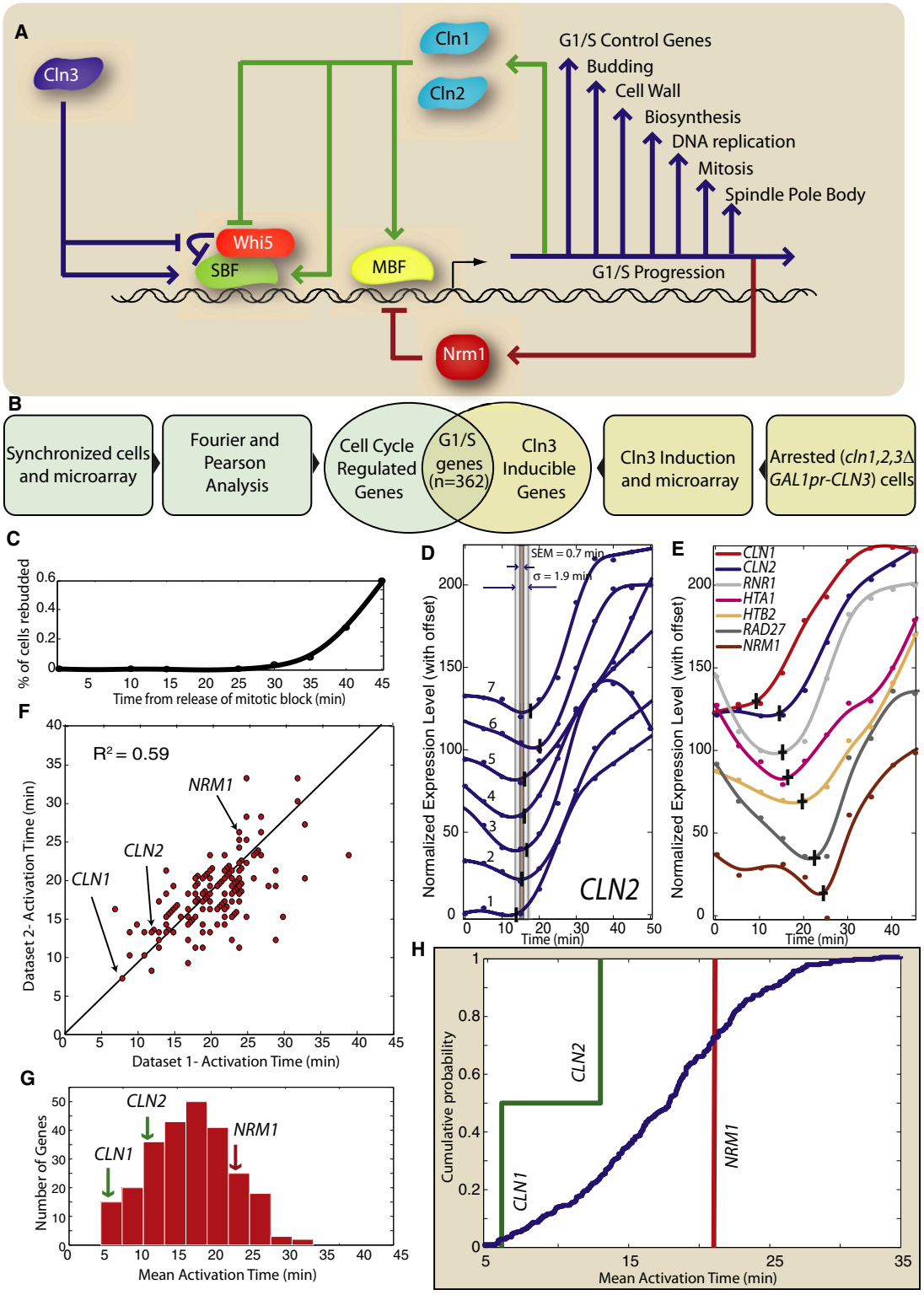

Figure 1. Positive Feedback Precedes Genome-wide Change in Transcription at G1/S in *S. cerevisiae*

(A) Schematic diagram of the G1/S transition.

(B) The G1/S regulon is defined as the intersection of the set of cell cycle-regulated genes with the set of Cln3-inducible genes.

genome-wide changes in transcription occur after commitment to division.

Although G1/S transcription is largely regulated by SBF and MBF, single-cell studies have revealed significant differences in transcriptional activation of the three regulon members *CLN2*, *RAD27*, and *RFA1* (Skotheim et al., 2008). A rapid, feedback-driven increase in CDK activity drives the coherent and nearly simultaneous induction of these three genes in WT cells. However, significant differences in transcriptional activation timing are revealed in *cln1Δ cln2Δ* cells lacking positive feedback. *CLN2* is induced earlier than two other regulon members, which suggests a model in which full regulon expression would only occur after feedback loop activation to avoid detrimental transcription in cases where the cell does not commit to the mitotic cell cycle. Therefore, we hypothesized that the G1 cyclins *CLN1* and *CLN2*, involved in positive feedback, would be activated earlier than other genes in the G1/S regulon to ensure that commitment precedes the genome-wide change in transcription.

In this study, we observed that the two SBF/MBF-regulated G1 cyclins, namely *CLN1* and *CLN2,* are among the earliest activated genes of the G1/S regulon, which supports the hypothesis that genome-wide changes in transcription occur after a cell is committed to division. By comparing sets of genes regulated by SBF, MBF, or by both factors together, we found that both transcriptional activation and inactivation can be approximated as logical OR functions. Furthermore, *CLN1* and *CLN2* remain among the earliest activated cell cycle-regulated genes in the related yeast, *S. bayanus*, which has significantly diverged gene expression (Tirosh et al., 2006; Guan et al., 2010). A similar analysis of human tissue culture cells revealed that functionally analogous feedback loop components *E2F1*, *Skp2*, and the *cyclins E1* and *E2* (Blagosklonny and Pardee 2002; Yung et al., 2007) are among the earliest activated cell cycle-regulated targets of the E2F family of transcription factors. Taken together, our results demonstrate that feedback-first regulation, which places genome-wide changes in transcription downstream of positive feedback-dependent cell-cycle commitment, is a common feature of G1/S control across eukaryotes.

RESULTS

Defining the G1/S Regulon

To test our model that induction of positive feedback and concomitant cell-cycle commitment precedes large-scale transcriptional change, we first need to accurately define the G1/S regulon. We are interested in the set of genes whose transcription is initiated due to increasing cyclin activity rather than upstream cyclin-independent processes (MacKay et al., 2001; Di Talia et al., 2009). The set of cell cycle-regulated genes was defined as the 800 genes with the largest amplitude messenger RNA (mRNA) concentration oscillation through the cell cycle (Spellman et al., 1998). To identify the set of G1 cyclin regulated genes, we relied on a second experiment by Spellman et al. (1998), which identified a set of genes responding to exogenous Cln3 induction in G1 arrested *cln1Δ cln2Δ cln3Δ* cells. We took the top 413 as the set of G1 cyclin inducible genes. The intersection of these two sets defines the 362-gene regulon (Figure 1B and Table S1 available online).

Automated Detection of Gene Activation

Next, we developed an algorithm to determine the time at which a specific gene is induced during the cell cycle. We analyzed seven previously published microarray time-course data sets with 5 min temporal resolution (Di Talia et al., 2009). All experiments were performed on *cdc20Δ GALLpr-CDC20* cells that were synchronized by mitotic arrest. Cells were released by switching to media containing galactose resulting in *CDC20* expression and a synchronous first cell cycle (Figure 1C).

Although manually identifying activation points of cell cycle-regulated genes is not difficult, we developed an automated algorithm to both avoid potential bias and increase throughput. Our algorithm is robust to noisy data, which can produce incorrect estimates for the activation time. We normalized all the time series and assumed that the time scale for changing transcript concentration is greater than 10 min. We therefore remove data points associated with large concentration changes on shorter timescales. Data points further than 20% of the dynamic range of the time series (maximum – minimum) from adjacent points are removed. We discarded time series with two or more removed data points. The mRNA level is then estimated with smoothing splines. We selected the point where the first derivative first reaches 10% of its maximum. The smoothing parameter is optimized to minimize variation in biological replicates and the first derivative method is shown to be superior in estimating activation times relative to other methods (Figures S1A–S1C).

Figure 1D shows the activation times for seven independent *CLN2* expression profiles and their standard deviation and standard error of the mean. Because we have multiple time courses, our error in estimating the activation time is low, e.g., for *CLN2* we find the activation time to be 13 min after galactose addition with a standard deviation of 1.9 min and a standard error of the mean of 0.7 min. For genes within the G1/S regulon, we find that the average standard deviation is 4.7 min and the average standard error of the mean is 2.1 min. Despite regulation by the same transcription factors, the activation times of G1/S regulon members

(C) Synchrony of *cdc20Δ GALLpr-CDC20* metaphase block-release from Di Talia et al. (2009).
(D) An algorithm is applied to a smoothing-spline fit to detect activation of *CLN2* transcription in seven mitotic block-release data sets (see Figures S1–S3 for algorithm description; specific genotypes of data sets 1–7 described in Figure S1D). The standard deviation σ and the standard error of the mean (SEM) are calculated for each gene.
(E) Seven genes in the G1/S regulon are activated at different times; data shown are from a single data set. The vertical and horizontal bars indicate the activation time and its SEM, respectively.
(F) Gene activation time correlation between two of the seven data sets ($R^2 = 0.59$; see the Supplemental Experimental Procedures for additional correlations).
(G and H) Histogram (G) and corresponding cumulative distribution (H) of mean activation times for the seven mitotic block-release data sets. *CLN1* and *CLN2*, two genes responsible for positive feedback, are among the earliest-activated genes. *NRM1*, a negative regulator of MBF, is activated later.
See also Figure S1, Table S1, and Table S2.

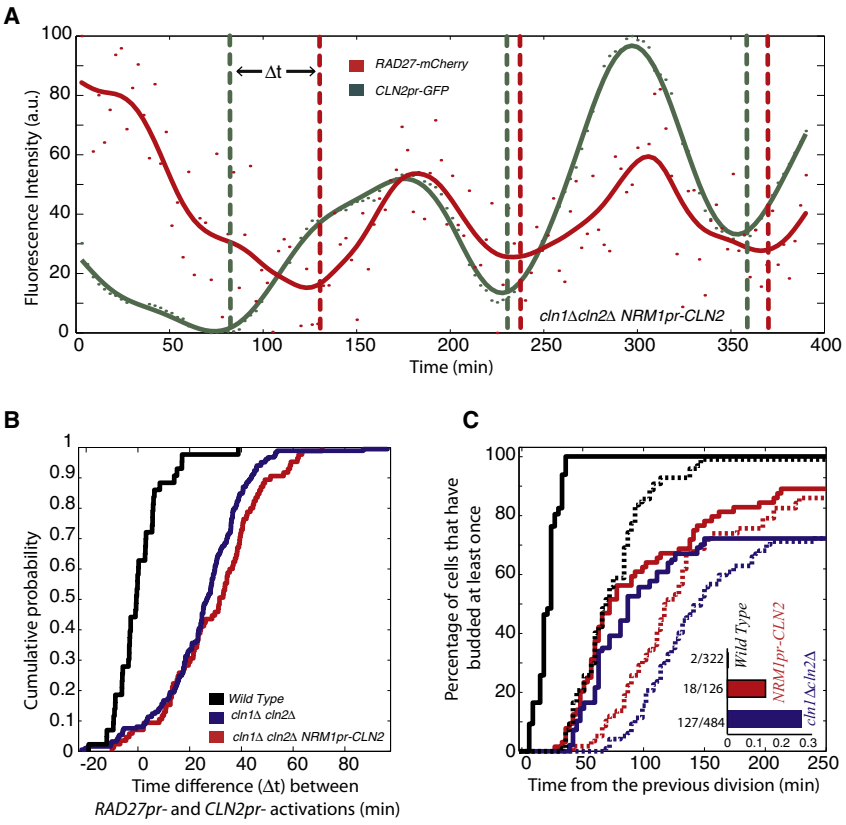

Figure 2. Phenotypic Consequences of Delayed Positive Feedback

(A) Time course of incoherent *RAD27-mCherry* and *CLN2pr-GFP* expression in a single *cln1Δ cln2Δ NRM1pr-CLN2* cell.

(B) Time difference between *CLN2pr* and *RAD27pr* induction measured as in Skotheim et al. (2008); cells not showing significant induction of either promoter were omitted from the analysis.

(C) A cumulative plot for the first bud emergence measured from cell division. Solid and dashed lines correspond to mother and daughter cells, respectively. Inset shows fraction of G1-arrested cells.

See also Figure S2.

has a defined distribution (mean = 17.2 min, standard deviation = 5.9 min; Figures 1E–1H, Figure S1D, and Table S2).

To test our model that feedback activation precedes regulon induction, we averaged the activation times from all seven data sets for each gene (Figures 1G and 1H). These results were consistent with induction times measured in real-time PCR time courses (see Figure S1E). The positive feedback genes *CLN1* and *CLN2* are activated significantly earlier than the bulk of the G1/S regulon. Indeed, within error, *CLN1* is the earliest activated gene, 5 min earlier than *CLN2*, suggesting a different temporal role even though these two genes are generally thought to be functionally redundant. However, it has been shown that *CLN1*, but not *CLN2*, transcription affects cell size (Flick et al., 1998), which our data suggests is due to timing. We note that for the feedback-first model to work it is sufficient to express either G1 cyclin, not necessarily both, prior to the majority of the regulon. Thus, we see that induction of the G1 cyclin positive feedback loop, which coincides with cell-cycle commitment, precedes large-scale changes in the transcriptional program.

Interestingly, *NRM1*, the negative feedback element responsible for inactivating MBF regulated genes (de Bruin et al., 2006), is activated 15 min later than *CLN1* (Figures 1G and 1H) even though both genes are MBF targets (Ferrezuelo et al., 2010). Thus, distinct temporal regulation allows positive feedback sufficient time for regulon transcription prior to *NRM1*-dependent inactivation.

Delayed Positive Feedback Does Not Rescue *cln1Δ cln2Δ* Cells

To examine the functional consequences of feedback timing, we integrated a *CLN2* allele regulated by the *NRM1* promoter into a *cln1Δ cln2Δ* cell containing *MET3pr-CLN2*, *CLN2pr-GFP*^{pest}, and *RAD27-mCherry*. Cells were grown overnight on media lacking methionine (*MET3pr-CLN2* on) prior to switching to media containing methionine (*MET3pr-CLN2* off) for single-cell analysis of one cell cycle (Skotheim et al., 2008). Cells exhibited similarly incoherent gene expression (time between *CLN2pr* and *RAD27pr* induction) and cell size defect as *cln1Δ cln2Δ* cells (Figures 2A and 2B and Figure S2). However, the fitness defect was partially reduced (Figure 2C). This indicates the importance of running the positive feedback loop from an early-activated promoter.

Feedback-First Regulation Is Robust to Changes in Carbon Source and Synchronization Method

To further test our feedback-first model, we examined the effects of varying carbon source and synchronization method, which are both known to affect gene expression (Flick et al., 1998; Levy et al., 2007; Brauer et al., 2008). We performed a microarray time course after synchronizing cells with mating pheromone in media with either glucose or galactose. Carbon source does not have a large effect, as differences in activation times were similar to experimental replicates (Figure 3A).

To analyze the effect of synchronization method, we examined cells lacking endogenous G1 cyclins (*cln1Δ cln2Δ cln3Δ*) but containing an integrated *MET3pr-CLN2* construct (see the Experimental Procedures). Cells were arrested in G1 before being transferred to media with a low level of methionine to activate exogenously controlled *CLN2* transcription at physiological levels. We then compared activation times between the cyclin blocked and the pheromone blocked cells (Figure 3B). Our three G1 block-release experiments varying carbon source and synchronization method produced similar timing profiles.

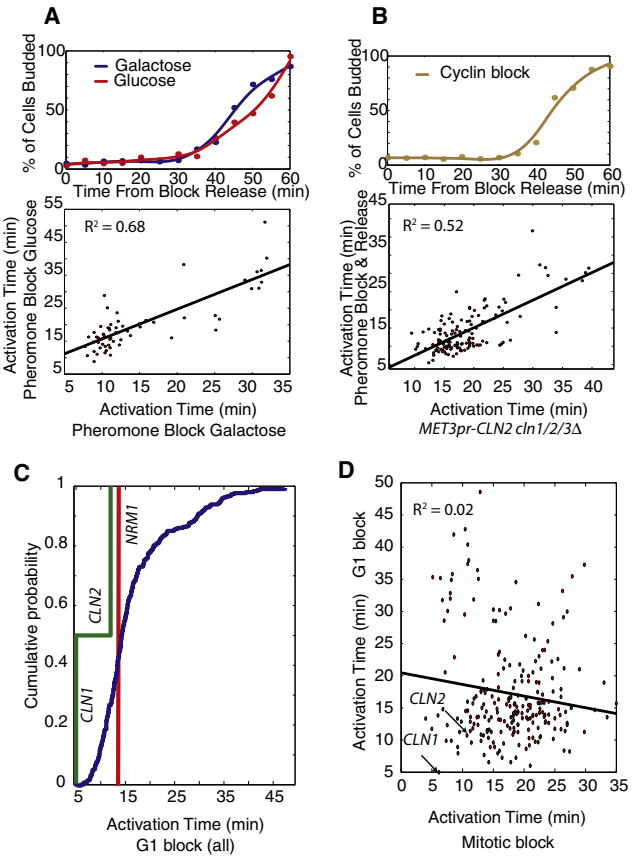

Figure 3. Synchronization Phase, but Not Carbon Source or Synchronization Method, Affects Gene Activation Timing

(A) Bud-index measurements and gene activation time correlation for G1 pheromone block-release time-course microarray experiments with glucose or galactose carbon sources.

(B) Bud index for G1 block-release usiwithng *cln1Δ cln2Δ cln3Δ MET3pr-CLN2* cells and correlation of gene activation times for pheromone and G1 cyclin block-release experiments.

(C) Significant correlation between the 3 G1 block-release datasets allows them to be pooled together to produce a histogram of accurately estimated activation times for the G1/S regulon again demonstrating feedback-first regulation.

(D) Activation times from G1 and mitotic block-release experiments are not correlated.

See also Figure S3 and Table S3.

We examined the distribution of activation times pooled from the three separate G1 block experiments (Figure 3C). Although transcriptional order is affected by the arrest phase (Figure 3D and Figure S3), *CLN1* is activated at the first possible time point (5 min after release) in agreement with the feedback-first model.

Gene Activation Is Correlated in Freely Cycling Cells and Mitotic Block-Release Experiments

Since transcriptional order changes with the arrest phase, we decided to investigate which block is more similar to the free-running cell cycle using time-lapse fluorescence microscopy (Skotheim et al., 2008). We analyzed protein accumulation in ten strains expressing C-terminal GFP fusion proteins from the endogenous loci (Ghaemmaghami et al., 2003) and two strains containing an integrated *CLN1* or *CLN2* promoter driving the expression of a destabilized $Venus_{PEST}$ (Mateus and Avery 2000). We selected this group of strains to span the distribution of activation times. Automated cell segmentation allows us to analyze the fluorescent intensity change in single cells through the cell cycle (Figure 4A). We detected activation timing relative to bud emergence (Figures 4B and 4C and Table S3). We found that the mean single-cell activation times in the unperturbed cell cycle correlated more with the mitotic block experiments (R^2 = 0.72; Figure 4D) than the G1 block experiments (R^2 = 0.21; Figure 4E). This result also implies that the order of mRNA transcription is largely reflected in protein accumulation. Thus, the mitotic block experiments are more representative of freely cycling cells.

Since transcription activation times change with the phase of the block used, we decided to analyze previously published cell cycle-synchronized microarray time courses (Spellman et al., 1998; Pramila et al., 2006; Orlando et al., 2008). Although quantitative comparisons of individual genes are difficult because of either poor temporal resolution or the lack of experimental replicates, we are able to detect correlations of genes within the G1/S regulon. We found that G1 blocks, including elutriation, correlate with our G1 block data (see Table S4). Interestingly, the $cdc15^{ts}$ data from Spellman et al. (1998) correlates with our G1 block experiments rather than the mitotic block experiments even though this is an anaphase block, indicating that an event occurring in cells blocked downstream of Cdc20 may be responsible for differences in gene activation timing. We note that release from G1 arrest and free cycling are both likely to be physiologically relevant.

SBF- and MBF-Dependent Activation Is a Logical OR Gate

We hypothesized that the observed differences in gene activation time in different blocks might be due to differential regulation of specific transcription factors. The majority of genes in what we defined as the G1/S regulon are regulated by the transcription factors SBF and MBF (Ferrezuelo et al., 2010). For our analysis, we divided the activation times of the G1/S genes into three categories: 136 SBF-only targets, 63 MBF-only targets, and 36 dual-regulated SBF and MBF targets.

Since combinatorial use of transcription factors may yield differential activation timing, we analyzed the activation times of the SBF only, MBF only, and dual-regulated genes. For our G1 arrest data, we find that MBF-only targets are activated earlier than SBF-only targets ($p < 0.01$). Furthermore, the distribution of the dual regulated targets is more similar to the earlier-activated MBF-only targets ($p = 0.90$) than the more tardy SBF-only targets ($p = 0.01$; Figure 5A).

In the mitotic block-release, the SBF-only targets are activated earlier than the MBF-only targets ($p = 0.08$). This is the opposite order than in the G1-block experiments and consistent with the lack of correlation between activation times of individual G1/S regulon members (Figure 3D). Furthermore, we find that the common targets are much more likely to follow the SBF-only distribution ($p = 0.79$) than the MBF-only distribution ($p = 0.06$; Figure 5B). We note that the SBF distribution is broader so that the late-activated SBF genes are activated later than the

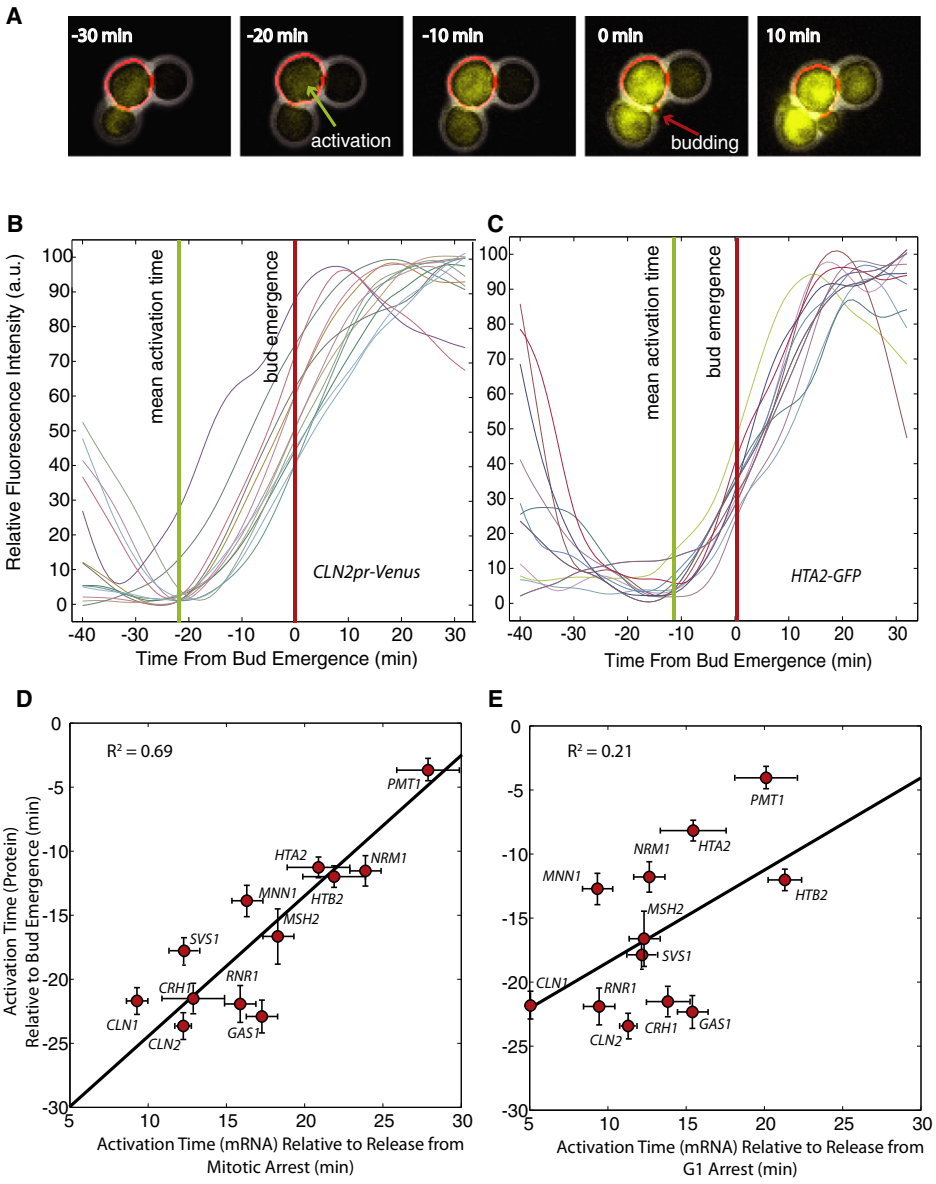

Figure 4. Gene Activation Is Correlated in the Free-Running Cell Cycle and Mitotic Block-Release Experiments

(A) Composite phase and fluorescence images of *CLN2pr-Venus*$_{PEST}$ cells. Venus yellow fluorescent protein contains a destabilizing PEST sequence. The red contour denotes the cell boundary detected by automatic segmentation.

(B and C) Gene activation time calculated from fluorescence intensity time courses aligned at bud emergence for (B) *CLN2pr-Venus*$_{PEST}$ and (C) *HTA2-GFP* cells.

(D and E) Gene activation times ± SEM for ten strains containing GFP-fused proteins and two strains containing promoter-Venus constructs expressed at the endogenous locus correlated with mean activation times from microarray time-courses for cells synchronized at mitosis (D) or G1 (E).

See also Tables S3 and S4.

late-activated MBF genes. However, the late-activated dual-regulated genes now appear to follow MBF.

Taken together, our results from the G1 and mitotic block-release experiments suggest that the dual-regulated targets are activated by the earliest active transcription factor. In the G1 block experiments, the coregulated genes are activated by MBF, while in the mitotic block experiments the co-regulated genes are activated by SBF. This implies that transcriptional activation is functioning as a logical OR gate, where either an active SBF or an active MBF is sufficient to activate transcription.

Logical Inactivation

Our results analyzing transcriptional activation encouraged us to perform a similar analysis on transcriptional inactivation, which we estimate as the time of the peak transcript level (Figure 5C). The peak time is defined to be the point where the first derivative

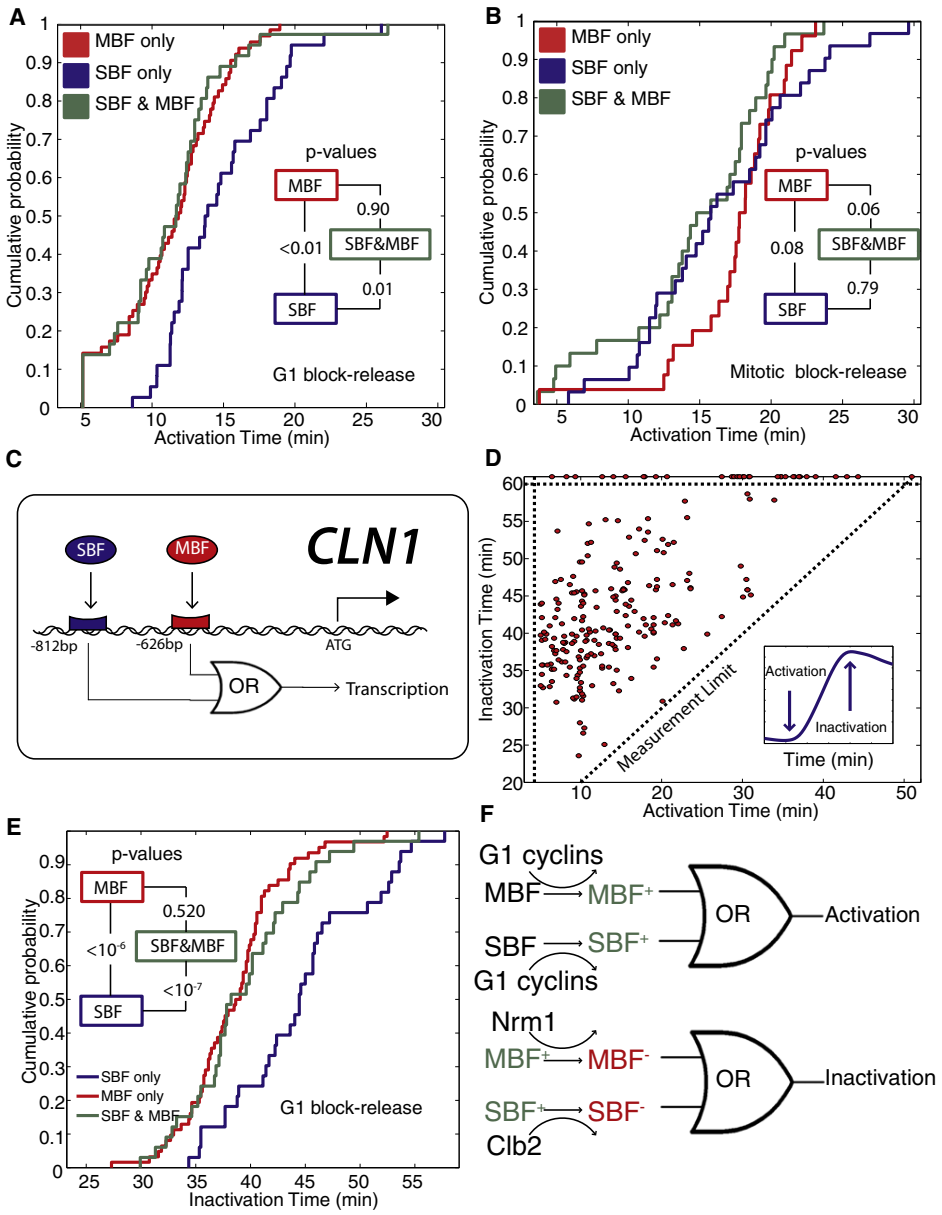

Figure 5. SBF and MBF Dual-Regulated Promoters Act as Logical OR Gates in Response to Activation and Inactivation Signals

(A and B) Cumulative probability of activation times for SBF-only, MBF-only, and SBF/MBF dual-regulated targets are plotted for G1 block-release (A) and mitotic block-release (B) experiments. Inset shows p values comparing each pair of distributions.

(C) Schematic showing logical regulation of the early-activated *CLN1* promoter denoting SBF and MBF consensus binding sites.

(D) Inactivation time for each gene, where the first derivative is zero and the second derivative is negative (inset), is uncorrelated with activation for G1 block-release experiments. Points above the horizontal dotted line represent genes peaking later than 60 min.

(E) Cumulative probability of inactivation for SBF-only, MBF-only, and SBF/MBF dual targets for G1 block-release experiments. Inset shows p values comparing each pair of distributions.

(F) The transcriptional activation and inactivation can be modeled as a logical OR gate. For dual-regulated genes, activating either SBF or MBF suffices for activation, while inactivating MBF suffices for inactivation. Different colors denote different possible states of a transcription factor.

of the smoothed data is zero and the second derivative is negative. We then implemented an algorithm for unbiased peak detection and analyzed our G1 block-release data. Inactivation is not well correlated with activation (Figure 5D).

Next, we decided to analyze inactivation in light of our SBF-only, MBF-only, and dual-regulated gene lists. Whereas mitotic cyclins are responsible for SBF inactivation (Amon et al., 1993), MBF inactivation is performed by Nrm1 possibly

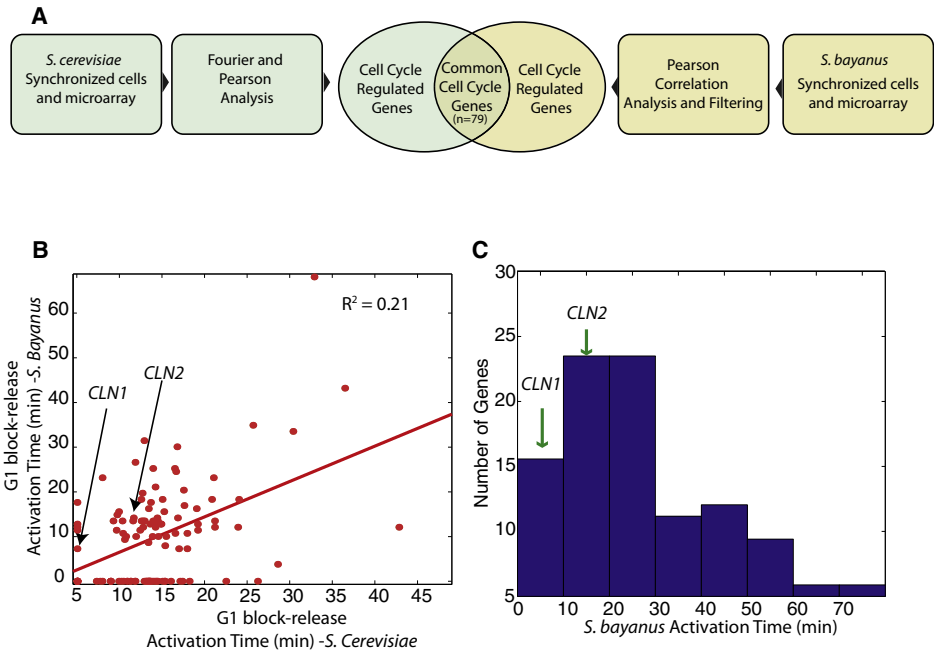

Figure 6. Feedback-First Regulation Is Conserved in the Budding Yeast *S. bayanus*

Activation times are analyzed for all cell cycle-regulated genes in a *S. bayanus* pheromone block-release microarray time-course (Guan et al., 2010).

(A) Intersection of cell cycle-regulated genes in both budding yeasts.

(B) Weak correlation between gene activation times in G1 block-release experiments for genes that are cell-cycle regulated in both *S. bayanus* and *S. cerevisiae*.

(C) Histogram of activation times of the cell cycle regulated genes in *S. bayanus* indicates that the G1 cyclins responsible for positive feedback, *CLN1* and *CLN2*, are among the early-activated genes.

through a direct interaction (de Bruin et al., 2006). In *nrm1Δ* cells, mitotic cyclins are capable of inactivating MBF-regulated genes; however, inactivation is delayed about 10 min relative to the WT (de Bruin et al., 2006). This suggests that mitotic cyclin-dependent inactivation occurs later than Nrm1-dependent inactivation and that we should expect to see MBF-only targets inactivated earlier than SBF-only targets. Consistent with previous results (Ferrezuelo et al., 2010), we find that MBF-only targets are inactivated earlier than SBF-only targets ($p < 10^{-7}$; Figure 5E and Figure S4). The distribution of inactivation times for the dual regulated genes was much more similar to the MBF-only genes ($p = 0.52$) than the SBF-only genes ($p < 10^{-7}$). Inactivation of MBF is sufficient to turn off gene expression regardless of the presence of an active SBF transcription factor. Thus, both activation and inactivation may be represented by logical OR gates (Figure 5F).

Feedback-First Regulation in the Budding Yeast *S. bayanus*

We found that *S. cerevisiae* activates positive feedback and commits to another round of cell division before making large-scale changes to its transcriptional program. This temporal organization of the G1/S regulon may be an efficient way to ensure that cell cycle-associated genes are only transcribed after a cell has decided to divide. If feedback-first regulation increases fitness then we should expect to see it conserved in divergent evolutionary lineages.

To examine the conservation of feedback-first regulation, we analyzed a closely related yeast *Saccharomyces bayanus*, for which cell cycle-synchronized microarray data were available. Compared to *S. cerevisiae*, *S. bayanus* has 67% local similarity of intergenic regions indicating significant divergence of gene regulation (Cliften et al., 2003). Gene orthologs are easily identified by sequence and the *S. bayanus* genes are conveniently annotated using the *S. cerevisiae* nomenclature (Cliften et al., 2003). Indeed, studies on the evolution of gene expression among *sensu stricto* yeast species revealed substantial differences (Tirosh et al., 2006; Guan et al., 2010).

We analyzed the *S. bayanus* time-course microarray data set from the GEO database (GSE16544). Cells were synchronized in G1 with mating pheromone, and samples were taken every 10 min for 300 min after release (Guan et al., 2010). To define a set of genes that are cell-cycle regulated, we calculated the cross-correlation coefficients with two known cell cycle-regulated genes, *CLN2* and the G2 gene *KIN2*. We sorted the genes based on their cross-correlation scores and selected the 714 genes that were in the top 1000 of both cross-correlations. To eliminate spurious profiles, we considered only genes showing multiple well-defined oscillations.

We analyzed the correlation of cell cycle-regulated gene expression in the two budding yeasts. Of the 800 and the 223 well-defined cell cycle-regulated genes in *S. cerevisiae* and *S. bayanus* respectively, only 79 were cell cycle-regulated in both species (Figure 6A). Furthermore, the activation times of

the common cell cycle-regulated genes is weakly correlated (R^2 = 0.22; Figure 6B). Our observation of significant changes in transcriptional activation timing through the cell cycle is consistent with the emerging picture of significantly diverged transcription across the *sensu stricto* (Tirosh et al., 2006).

To test for the conservation of feedback-first regulation, we analyzed the distribution of first activation times (<80 min). The activation times for *CLN1* and *CLN2* was calculated to be 6 and 15 min, respectively. Thus, the G1 cyclins are among the earliest activated genes in the *S. bayanus* cell cycle, which indicates conservation of feedback-first regulation (Figure 6C).

Temporal Analysis of E2F-Dependent Transcription in Human Cells

Our finding that two yeasts engage positive feedback prior to full regulon activation suggests that this regulatory motif is widespread. Thus, we chose to examine a mammalian system. Although many of the components of the genetic network regulating the G1/S transition in mammals do not have well-defined orthologs in yeast, both networks contain multiple positive feedback elements indicating similar network topology (Figure 7A). There is a functional analogy between the cyclin D-E2F-Rb-cyclinE and the Cln3-SBF/MBF-Whi5-Cln1/2 pathways. Furthermore, both budding yeasts and mammals regulate commitment to cell division in response to multiple internal and external signals at the G1/S transition (Planas-Silva and Weinberg 1997; Blagosklonny and Pardee 2002; Yao et al., 2008).

Mammalian G1 progression is initiated by mitogen-dependent activation of cyclin D-CDK4/6 complexes, which phosphorylate and partially inactivate the transcriptional inhibitor Rb (Blagosklonny and Pardee 2002). This allows for the activation of transcription by three members of the E2F family (E2F1-3) of transcription factors. Included in the set of targeted genes are the cyclins E1 and E2, which complex with CDK2 to phosphorylate Rb and thereby complete a positive feedback loop (Bracken et al., 2004). Additionally, E2F1-3 activate transcription of *E2F1*, which may form an additional transcriptional positive feedback loop (Johnson et al., 1994). The SCF component Skp2, responsible for the specific degradation of the CDK inhibitor p27, is also an E2F target (Yung et al., 2007). Therefore, multiple potential positive feedback loops may act during the mammalian G1/S transition. If our feedback-first model applies to mammalian cell-cycle control, we expect to see feedback loop components transcribed before other E2F targets.

To test our hypothesis that the positive feedback elements are transcribed early, we first need to define a set of cell cycle-regulated E2F targets (Markey et al., 2002; Ren et al., 2002). Therefore, we compiled a list of 315 cell cycle-regulated E2F targets from previous studies (Müller et al., 2001; Whitfield et al., 2002; Xu et al., 2007).

We analyzed gene activation timing in human HeLa cells for four cell cycle-synchronized microarray time courses (Whitfield et al., 2002). We see consistent activation of individual genes across the data sets. For example, *cyclin E1* is activated at 5.9 ± 0.5 hr on average with a standard deviation of 1.1 hr (Figure 7B). Our analysis identifies distinct activation times for E2F regulated genes (Figure 7C). In three experiments, cells were synchronized with a double thymidine block, while in one experiment, cells were synchronized with a thymidine block followed by a nocodazole block (Whitfield et al., 2002). However, we see no difference in relative activation timing due to the two different synchronization methods as all four data sets yield comparable results (Figure 7D). We observe that genes responsible for positive feedback (*cyclin E1*, *cyclin E2*, *Skp2*, and *E2F1*) are among the first transcribed at the G1/S transition consistent with our feedback-first model (Figure 7E).

DISCUSSION

We showed that genome-wide transcription is restricted until positive feedback commits a cell to division. This regulatory organization was previously unclear because transcription of the G1 cyclins and the rest of the G1/S regulon are both dependent on the same transcription factors and appear concurrent when analyzed with clustering-based algorithms. In contrast to clustering methods, both our activation detection algorithm and parametric algorithms preserve the dynamic information required for our analysis (Chechik et al., 2008).

Toward the Mechanistic Basis of Transcription Order

We observed considerable variation in gene activation timing among genes regulated by a specific transcription factor. In budding yeast, we showed that a significant amount of this variation is due to combinatorial use of the transcription factors SBF and MBF resulting in logical OR gates for both transcriptional activation and inactivation. Thus, the genes regulated by both SBF and MBF transcription factors are activated early in mitotic block-release experiments, where SBF is activated before MBF, and in G1 block-release experiments, where MBF is activated before SBF. This may be functionally relevant as the earliest activated G1 cyclin *CLN1* is regulated by both factors (Flick et al., 1998; Ferrezuelo et al., 2010), which may ensure feedback-first regulation in a variety of physiological contexts.

Future work will aim at explaining the molecular basis for the significant temporal variation in G1/S transcription unexplained by the combinatorial use of SBF and MBF. One possibility is that differential transcription timing may arise through the combinatorial use of additional transcription factors (Kato et al., 2004). In such a model, intermediate times might be produced by regulating a promoter with a late-activated and an early-activated transcription factor. An example of this type of regulation is that the Fkh2-regulated genes show different activation times at G2/M depending on Yox1 coregulation (Darieva et al., 2010). This model suggests that the late activated SBF targets might also be regulated by a late-activated transcription factor such as Fkh2. A large number of transcription factors might therefore account for the variation in gene activation time.

A second possibility is that promoter-specific rate-constants underlie gene activation kinetics. This could arise through promoter-specific transcription factor and nucleosome arrangements or TATA-box sequence (Lam et al., 2008; Chechik and Koller 2009; Bai et al., 2010; Mogno et al., 2010). Thus, in response to a single input such as CDK activity, the organization

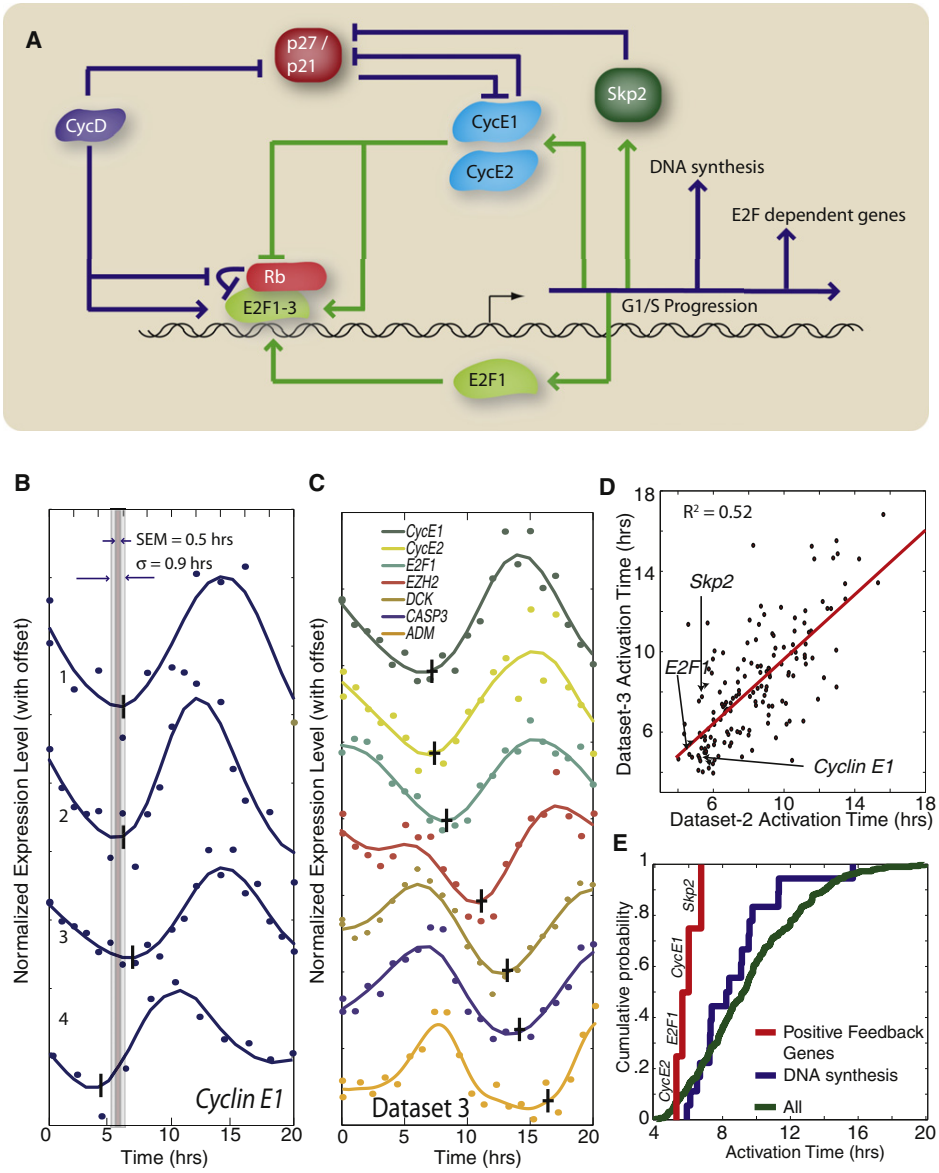

Figure 7. Feedback-First Regulation Is Conserved in Human Cells

(A) Schematic diagram of G1/S regulation in human cells.

(B) *cyclin E1* activation is consistent in four different cell cycle-synchronized microarray experiments from Whitfield et al. (2002). The standard deviation σ and the SEM are calculated for each gene.

(C) Seven genes regulated by the E2F family of transcription factors are activated at different times; data shown are from a single data set. The vertical and horizontal bars indicate the mean activation time and the SEM, respectively.

(D) Gene activation time correlation between two data sets ($R^2 = 0.52$).

(E) Cumulative distribution of mean activation times for cell cycle-regulated E2F targets. Genes responsible for positive feedback at the G1/S transition, including the *cyclins E1* and E2 the transcription factor *E2F1*, and the SCF component *Skp2*, are transcribed earlier than other E2F targets ($p < 0.01$) and earlier than the set of E2F targets specifically involved in DNA replication ($p = 0.03$). This demonstrates the conservation of feedback-first regulation in eukaryotes.

See also Table S5.

of kinetic parameters can result in differential activation timing (Shen-Orr et al., 2002). We note that these two classes of mechanisms are not mutually exclusive and likely cooperate to tune gene expression.

Temporal Separation of Positive and Negative Feedback Loops

An interesting feature of the G1/S regulon is that both positive (*CLN1,2*) and negative (*NRM1*) feedback elements are regulated

under the same CDK-dependent transcription factors. Activation of both feedbacks at the same time would be much like stepping on the brake and gas pedals simultaneously to detrimental effect (Figure 2). To avoid this outcome, promoter-specific kinetics may allow temporal separation of positive and negative feedback loops. A similar process was found to regulate mitotic entry in *Xenopus* egg extracts (Georgi et al., 2002). Wee1 and Cdc25 phosphorylation by CDK1, which is associated with positive feedback at mitotic entry, occurs before the phosphorylation of other CDK1 targets including the APC component Cdc27. Thus, both feedback-first regulation and the temporal separation of positive and negative feedback loops may be enacted through the evolution of differential rate constants.

Feedback-First Regulation Ensures Commitment to Cell Division prior to Large-Scale Changes in Gene Expression

Transcribing genes when they are needed may increase efficiency by avoiding unnecessary protein synthesis. The subunits of the *E. coli* flagella were found to be synthesized in the order that they are needed for assembly (Kalir et al., 2001). Fine temporal control of transcription during amino acid synthesis ensured that enzymes were made in the order they were needed (Zaslaver et al., 2004). In the cell-cycle context, ribonucleotide reductase is transcribed just before S phase (Elledge and Davis 1990), and histones are transcribed during S phase to be assembled with newly replicated DNA (Borun et al., 1975; Hereford et al., 1981). Taken together, these studies indicate that fine temporal order of events may provide a fitness advantage.

A transcriptional oscillation with specific temporal order occurs through the cell division cycle in both prokaryotes and eukaryotes. This extensive oscillation entails ~10%–20% of all *Caulobacter* and budding-yeast genes (Cho et al., 1998; Spellman et al., 1998; Laub et al., 2000). However, a comparative analysis of the yeasts *S. pombe* and *S. cerevisiae* revealed that temporal regulation of most orthologous genes is not well conserved (Rustici et al., 2004; Oliva et al., 2005; Peng et al., 2005). Indeed, we report here that the order of gene activation at the G1/S transition in *S. cerevisiae* depends on the synchronization phase (Figure 3D). Further comparison of the two yeasts with human cell lines and the plant *Arabidopsis* revealed that only five orthologs are cell-cycle regulated in all four species (Jensen et al., 2006). However, different protein subunits of the same complex were often found to have cell cycle-regulated transcription in different species, suggesting conserved transcriptional control of the complex rather than the individual subunits (Jensen et al., 2006). Thus, although periodic transcription of individual genes varies, there may still be conserved regulatory features.

Here, we identify such a conserved regulatory feature of the eukaryotic cell cycle. We find that commitment via positive feedback precedes large-scale transcriptional activation at the G1/S transition. Our study was able to identify feedback-first regulation because we employ an algorithm to analyze activation and inactivation separately. We revealed feedback-first regulation in the yeasts, *S. cerevisiae* and *S. bayanus* as well as in human cells. The conservation of feedback-first regulation leads us to anticipate its widespread use in cellular and developmental transitions.

EXPERIMENTAL PROCEDURES

Microarray Experiments and Analysis

Mitotic block-release analysis was based on data collected in (Di Talia et al., 2009). The sequential order of activations is highly consistent between datasets indicating a defined temporal regulation even though the genotypes for the seven time courses were not identical (Figure 1F, Figure S1D, and Table S2).

G1 block-release experiments were performed at 30°C. Cells were harvested immediately after inoculation and then every 5 min thereafter. Microarray hybridization was performed at the SUNY Stony Brook Microarray Facility. For pheromone block experiments, *bar1Δ* cells were grown in log phase in either SCD (%2) or SCG (3%) before being arrested for 135 min in 95 nM α factor. Cells were then washed and inoculated into pheromone-free media. The cln-block experiment was performed with *cln1Δ cln2Δ cln3Δ MET3pr-CLN2* cells grown to early log phase in SCD – met (media without methionine; exogenous *CLN2* on), then 0.2 g/liter met was added for 120 min to arrest cells in early G1 (*CLN2* off). Cells were then washed and inoculated into 4 mg/liter met (*CLN2* partially on) to provide the amount of *CLN2* expression resulting in budding kinetics similar to WT cells released from a pheromone block.

There was some ambiguity in identifying the gene activation time for *CLN1* in the *S. bayanus* data set because either the second or third data point for *CLN1* was likely an outlier. Therefore, we averaged the activation times for the dataset after having removed either the second or third data point.

Time-Lapse Fluorescence Microscopy

Wide-field fluorescence and phase-contrast images were captured every 3 min for 6 hr from cells prepared as previously described (Bean et al., 2006). Cells were automatically segmented and the mean fluorescence intensity was measured. Bud emergence was identified manually with phase images.

ACCESSION NUMBERS

The GEO accession number for the G1 block-release microarray data reported in this paper is GSE29894.

SUPPLEMENTAL INFORMATION

Supplemental Information includes Supplemental Experimental Procedures, four figures, and five tables and can be found with this article online at doi:10.1016/j.molcel.2011.06.024.

ACKNOWLEDGMENTS

We thank Chris Aakre, Amanda Amodeo, Lucy Bai, Fred Cross, Stefano Di Talia, Bruce Futcher, Amy Gladfelter, and Eric Siggia for insightful discussions and comments on the manuscript. The Burroughs Wellcome Fund, the National Institutes of Health (GM092925), and the National Science Foundation (CAREER award #1054025) supported this research.

Received: December 15, 2010
Revised: April 13, 2011
Accepted: June 17, 2011
Published: August 18, 2011

REFERENCES

Amon, A., Tyers, M., Futcher, B., and Nasmyth, K. (1993). Mechanisms that help the yeast cell cycle clock tick: G2 cyclins transcriptionally activate G2 cyclins and repress G1 cyclins. Cell *74*, 993–1007.

Andrews, B.J., and Herskowitz, I. (1989). Identification of a DNA binding factor involved in cell-cycle control of the yeast HO gene. Cell *57*, 21–29.

Bai, L., Charvin, G., Siggia, E.D., and Cross, F.R. (2010). Nucleosome-depleted regions in cell-cycle-regulated promoters ensure reliable gene expression in every cell cycle. Dev. Cell *18*, 544–555.

Bean, J.M., Siggia, E.D., and Cross, F.R. (2006). Coherence and timing of cell cycle start examined at single-cell resolution. Mol. Cell *21*, 3–14.

Blagosklonny, M.V., and Pardee, A.B. (2002). The restriction point of the cell cycle. Cell Cycle *1*, 103–110.

Borun, T.W., Gabrielli, F., Ajiro, K., Zweidler, A., and Baglioni, C. (1975). Further evidence of transcriptional and translational control of histone messenger RNA during the HeLa S3 cycle. Cell *4*, 59–67.

Bracken, A.P., Ciro, M., Cocito, A., and Helin, K. (2004). E2F target genes: unraveling the biology. Trends Biochem. Sci. *29*, 409–417.

Brauer, M.J., Huttenhower, C., Airoldi, E.M., Rosenstein, R., Matese, J.C., Gresham, D., Boer, V.M., Troyanskaya, O.G., and Botstein, D. (2008). Coordination of growth rate, cell cycle, stress response, and metabolic activity in yeast. Mol. Biol. Cell *19*, 352–367.

Chechik, G., and Koller, D. (2009). Timing of gene expression responses to environmental changes. J. Comput. Biol. *16*, 279–290.

Chechik, G., Oh, E., Rando, O., Weissman, J., Regev, A., and Koller, D. (2008). Activity motifs reveal principles of timing in transcriptional control of the yeast metabolic network. Nat. Biotechnol. *26*, 1251–1259.

Cho, R.J., Campbell, M.J., Winzeler, E.A., Steinmetz, L., Conway, A., Wodicka, L., Wolfsberg, T.G., Gabrielian, A.E., Landsman, D., Lockhart, D.J., and Davis, R.W. (1998). A genome-wide transcriptional analysis of the mitotic cell cycle. Mol. Cell *2*, 65–73.

Cliften, P., Sudarsanam, P., Desikan, A., Fulton, L., Fulton, B., Majors, J., Waterston, R., Cohen, B.A., and Johnston, M. (2003). Finding functional features in Saccharomyces genomes by phylogenetic footprinting. Science *301*, 71–76.

Costanzo, M., Nishikawa, J.L., Tang, X., Millman, J.S., Schub, O., Breitkreuz, K., Dewar, D., Rupes, I., Andrews, B., and Tyers, M. (2004). CDK activity antagonizes Whi5, an inhibitor of G1/S transcription in yeast. Cell *117*, 899–913.

Darieva, Z., Clancy, A., Bulmer, R., Williams, E., Pic-Taylor, A., Morgan, B.A., and Sharrocks, A.D. (2010). A competitive transcription factor binding mechanism determines the timing of late cell cycle-dependent gene expression. Mol. Cell *38*, 29–40.

de Bruin, R.A., McDonald, W.H., Kalashnikova, T.I., Yates, J., 3rd, and Wittenberg, C. (2004). Cln3 activates G1-specific transcription via phosphorylation of the SBF bound repressor Whi5. Cell *117*, 887–898.

de Bruin, R.A., Kalashnikova, T.I., Chahwan, C., McDonald, W.H., Wohlschlegel, J., Yates, J., 3rd, Russell, P., and Wittenberg, C. (2006). Constraining G1-specific transcription to late G1 phase: the MBF-associated corepressor Nrm1 acts via negative feedback. Mol. Cell *23*, 483–496.

Di Talia, S., Wang, H., Skotheim, J.M., Rosebrock, A.P., Futcher, B., and Cross, F.R. (2009). Daughter-specific transcription factors regulate cell size control in budding yeast. PLoS Biol. *7*, e1000221.

Dirick, L., Böhm, T., and Nasmyth, K. (1995). Roles and regulation of Cln-Cdc28 kinases at the start of the cell cycle of Saccharomyces cerevisiae. EMBO J. *14*, 4803–4813.

Dončić, A., Falleur-Fettig, M., and Skotheim, J.M. (2011). Distinct interactions select and maintain a specific cell fate. Mol. Cell *43*, this issue, 528–539.

Elledge, S.J., and Davis, R.W. (1990). Two genes differentially regulated in the cell cycle and by DNA-damaging agents encode alternative regulatory subunits of ribonucleotide reductase. Genes Dev. *4*, 740–751.

Ferrezuelo, F., Colomina, N., Futcher, B., and Aldea, M. (2010). The transcriptional network activated by Cln3 cyclin at the G1-to-S transition of the yeast cell cycle. Genome Biol. *11*, R67.

Flick, K., Chapman-Shimshoni, D., Stuart, D., Guaderrama, M., and Wittenberg, C. (1998). Regulation of cell size by glucose is exerted via repression of the CLN1 promoter. Mol. Cell. Biol. *18*, 2492–2501.

Georgi, A.B., Stukenberg, P.T., and Kirschner, M.W. (2002). Timing of events in mitosis. Curr. Biol. *12*, 105–114.

Ghaemmaghami, S., Huh, W.K., Bower, K., Howson, R.W., Belle, A., Dephoure, N., O'Shea, E.K., and Weissman, J.S. (2003). Global analysis of protein expression in yeast. Nature *425*, 737–741.

Guan, Y., Dunham, M., Caudy, A., and Troyanskaya, O. (2010). Systematic planning of genome-scale experiments in poorly studied species. PLoS Comput. Biol. *6*, e1000698.

Hartwell, L.H., and Weinert, T.A. (1989). Checkpoints: controls that ensure the order of cell cycle events. Science *246*, 629–634.

Hartwell, L.H., Culotti, J., Pringle, J.R., and Reid, B.J. (1974). Genetic control of the cell division cycle in yeast. Science *183*, 46–51.

Hereford, L.M., Osley, M.A., Ludwig, T.R., 2nd, and McLaughlin, C.S. (1981). Cell-cycle regulation of yeast histone mRNA. Cell *24*, 367–375.

Holt, L.J., Krutchinsky, A.N., and Morgan, D.O. (2008). Positive feedback sharpens the anaphase switch. Nature *454*, 353–357.

Jensen, L.J., Jensen, T.S., de Lichtenberg, U., Brunak, S., and Bork, P. (2006). Co-evolution of transcriptional and post-translational cell-cycle regulation. Nature *443*, 594–597.

Johnson, D.G., Ohtani, K., and Nevins, J.R. (1994). Autoregulatory control of E2F1 expression in response to positive and negative regulators of cell cycle progression. Genes Dev. *8*, 1514–1525.

Justman, Q.A., Serber, Z., Ferrell, J.E., Jr., El-Samad, H., and Shokat, K.M. (2009). Tuning the activation threshold of a kinase network by nested feedback loops. Science *324*, 509–512.

Kalir, S., McClure, J., Pabbaraju, K., Southward, C., Ronen, M., Leibler, S., Surette, M.G., and Alon, U. (2001). Ordering genes in a flagella pathway by analysis of expression kinetics from living bacteria. Science *292*, 2080–2083.

Kato, M., Hata, N., Banerjee, N., Futcher, B., and Zhang, M.Q. (2004). Identifying combinatorial regulation of transcription factors and binding motifs. Genome Biol. *5*, R56.

Koch, C., Moll, T., Neuberg, M., Ahorn, H., and Nasmyth, K. (1993). A role for the transcription factors Mbp1 and Swi4 in progression from G1 to S phase. Science *261*, 1551–1557.

Lam, F.H., Steger, D.J., and O'Shea, E.K. (2008). Chromatin decouples promoter threshold from dynamic range. Nature *453*, 246–250.

Laub, M.T., McAdams, H.H., Feldblyum, T., Fraser, C.M., and Shapiro, L. (2000). Global analysis of the genetic network controlling a bacterial cell cycle. Science *290*, 2144–2148.

Levy, S., Ihmels, J., Carmi, M., Weinberger, A., Friedlander, G., and Barkai, N. (2007). Strategy of transcription regulation in the budding yeast. PLoS ONE *2*, e250.

López-Avilés, S., Kapuy, O., Novák, B., and Uhlmann, F. (2009). Irreversibility of mitotic exit is the consequence of systems-level feedback. Nature *459*, 592–595.

MacKay, V.L., Mai, B., Waters, L., and Breeden, L.L. (2001). Early cell cycle box-mediated transcription of CLN3 and SWI4 contributes to the proper timing of the G(1)-to-S transition in budding yeast. Mol. Cell. Biol. *21*, 4140–4148.

Markey, M.P., Angus, S.P., Strobeck, M.W., Williams, S.L., Gunawardena, R.W., Aronow, B.J., and Knudsen, E.S. (2002). Unbiased analysis of RB-mediated transcriptional repression identifies novel targets and distinctions from E2F action. Cancer Res. *62*, 6587–6597.

Mateus, C., and Avery, S.V. (2000). Destabilized green fluorescent protein for monitoring dynamic changes in yeast gene expression with flow cytometry. Yeast *16*, 1313–1323.

Mogno, I., Vallania, F., Mitra, R.D., and Cohen, B.A. (2010). TATA is a modular component of synthetic promoters. Genome Res. *20*, 1391–1397.

Morgan, D.O. (2007). The Cell Cycle: Principles of Control (London; Sunderland, MA: New Science Press; Sinauer Associates).

Müller, H., Bracken, A.P., Vernell, R., Moroni, M.C., Christians, F., Grassilli, E., Prosperini, E., Vigo, E., Oliner, J.D., and Helin, K. (2001). E2Fs regulate the

expression of genes involved in differentiation, development, proliferation, and apoptosis. Genes Dev. *15*, 267–285.

Nasmyth, K., and Dirick, L. (1991). The role of SWI4 and SWI6 in the activity of G1 cyclins in yeast. Cell *66*, 995–1013.

Oliva, A., Rosebrock, A., Ferrezuelo, F., Pyne, S., Chen, H., Skiena, S., Futcher, B., and Leatherwood, J. (2005). The cell cycle-regulated genes of Schizosaccharomyces pombe. PLoS Biol. *3*, e225.

Orlando, D.A., Lin, C.Y., Bernard, A., Wang, J.Y., Socolar, J.E., Iversen, E.S., Hartemink, A.J., and Haase, S.B. (2008). Global control of cell-cycle transcription by coupled CDK and network oscillators. Nature *453*, 944–947.

Peng, X., Karuturi, R.K., Miller, L.D., Lin, K., Jia, Y., Kondu, P., Wang, L., Wong, L.S., Liu, E.T., Balasubramanian, M.K., and Liu, J. (2005). Identification of cell cycle-regulated genes in fission yeast. Mol. Biol. Cell *16*, 1026–1042.

Planas-Silva, M.D., and Weinberg, R.A. (1997). The restriction point and control of cell proliferation. Curr. Opin. Cell Biol. *9*, 768–772.

Pomerening, J.R., Sontag, E.D., and Ferrell, J.E., Jr. (2003). Building a cell cycle oscillator: hysteresis and bistability in the activation of Cdc2. Nat. Cell Biol. *5*, 346–351.

Pramila, T., Wu, W., Miles, S., Noble, W.S., and Breeden, L.L. (2006). The Forkhead transcription factor Hcm1 regulates chromosome segregation genes and fills the S-phase gap in the transcriptional circuitry of the cell cycle. Genes Dev. *20*, 2266–2278.

Ren, B., Cam, H., Takahashi, Y., Volkert, T., Terragni, J., Young, R.A., and Dynlacht, B.D. (2002). E2F integrates cell cycle progression with DNA repair, replication, and G(2)/M checkpoints. Genes Dev. *16*, 245–256.

Rustici, G., Mata, J., Kivinen, K., Lió, P., Penkett, C.J., Burns, G., Hayles, J., Brazma, A., Nurse, P., and Bähler, J. (2004). Periodic gene expression program of the fission yeast cell cycle. Nat. Genet. *36*, 809–817.

Shen-Orr, S.S., Milo, R., Mangan, S., and Alon, U. (2002). Network motifs in the transcriptional regulation network of Escherichia coli. Nat. Genet. *31*, 64–68.

Skotheim, J.M., Di Talia, S., Siggia, E.D., and Cross, F.R. (2008). Positive feedback of G1 cyclins ensures coherent cell cycle entry. Nature *454*, 291–296.

Spellman, P.T., Sherlock, G., Zhang, M.Q., Iyer, V.R., Anders, K., Eisen, M.B., Brown, P.O., Botstein, D., and Futcher, B. (1998). Comprehensive identification of cell cycle-regulated genes of the yeast Saccharomyces cerevisiae by microarray hybridization. Mol. Biol. Cell *9*, 3273–3297.

Stuart, D., and Wittenberg, C. (1995). CLN3, not positive feedback, determines the timing of CLN2 transcription in cycling cells. Genes Dev. *9*, 2780–2794.

Tirosh, I., Weinberger, A., Carmi, M., and Barkai, N. (2006). A genetic signature of interspecies variations in gene expression. Nat. Genet. *38*, 830–834.

Tyers, M., Tokiwa, G., and Futcher, B. (1993). Comparison of the Saccharomyces cerevisiae G1 cyclins: Cln3 may be an upstream activator of Cln1, Cln2 and other cyclins. EMBO J. *12*, 1955–1968.

Whitfield, M.L., Sherlock, G., Saldanha, A.J., Murray, J.I., Ball, C.A., Alexander, K.E., Matese, J.C., Perou, C.M., Hurt, M.M., Brown, P.O., and Botstein, D. (2002). Identification of genes periodically expressed in the human cell cycle and their expression in tumors. Mol. Biol. Cell *13*, 1977–2000.

Wijnen, H., Landman, A., and Futcher, B. (2002). The G(1) cyclin Cln3 promotes cell cycle entry via the transcription factor Swi6. Mol. Cell. Biol. *22*, 4402–4418.

Xiong, W., and Ferrell, J.E., Jr. (2003). A positive-feedback-based bistable 'memory module' that governs a cell fate decision. Nature *426*, 460–465.

Xu, X., Bieda, M., Jin, V.X., Rabinovich, A., Oberley, M.J., Green, R., and Farnham, P.J. (2007). A comprehensive ChIP-chip analysis of E2F1, E2F4, and E2F6 in normal and tumor cells reveals interchangeable roles of E2F family members. Genome Res. *17*, 1550–1561.

Yao, G., Lee, T.J., Mori, S., Nevins, J.R., and You, L. (2008). A bistable Rb-E2F switch underlies the restriction point. Nat. Cell Biol. *10*, 476–482.

Yung, Y., Walker, J.L., Roberts, J.M., and Assoian, R.K. (2007). A Skp2 autoinduction loop and restriction point control. J. Cell Biol. *178*, 741–747.

Zaslaver, A., Mayo, A.E., Rosenberg, R., Bashkin, P., Sberro, H., Tsalyuk, M., Surette, M.G., and Alon, U. (2004). Just-in-time transcription program in metabolic pathways. Nat. Genet. *36*, 486–491.

Molecular Cell, *Volume 43*

Supplemental Information

Commitment to a Cellular Transition

Precedes Genome-wide Transcriptional Change

Umut Eser, Melody Falleur-Fettig, Amy Johnson, and Jan M. Skotheim

Contents

Supplemental Experimental Procedures

Algorithm to Find the Gene Activation Time

Although manually identifying activation points of cell cycle regulated genes is not difficult, we developed an automated activation time finder program to avoid potential bias and increase throughput.

The change in concentration of an mRNA species, ***dX(t)/dt***, depends on a balance between the transcription rate, ***r(t)***, and degradation rate, ***λX(t)***, so that

$$\frac{dX(t)}{dt} = r(t) - \lambda X(t) \quad (1)$$

Here, we want to find the time point where ***r(t)*** increases rapidly, i.e., the activation time. For cell cycle dependent changes in r, the timescale of mRNA degradation (~20min)(Grigull 2004) is more rapid than the cell cycle timescale (>90 minutes) so that we may neglect degradation kinetics around the time of gene activation (***λX(t) << r***) and consider the point where ***dX/dt*** increases above a threshold as the activation point (r > threshold). Hence, we define the activation time as the time point where the first derivative of the expression profile, ***dX/dt,*** reaches the defined threshold, which we take as 10% of the maximum value of the 1st derivative within a given time series. Alternatively, we can consider the value where the second derivative ***d^2X/dt^2*** is maximum as the activation point, *i.e.*, where the increase in transcription rate is most rapid (2nd derivative method)(Skotheim, Di Talia et al. 2008). Since both the 1st derivative and 2nd derivative can be used to estimate activation, we must rationally choose between methods.

Since noisy data can produce incorrect estimates for the activation time, we require a systematic method to exclude outlying data points and discard low-quality time series. Because the time scale for changing transcript concentration is greater than 10 minutes, we remove data points associated with large concentration changes on shorter time scales. If a data point is more than 20% of the dynamic range of the time series (maximum – minimum), away from both the adjacent points, it is removed. We discarded time series where two or more points removed or missing from the original data.

To estimate ***X(t),*** we applied smoothing-spline function by using the Curve Fitting Toolbox in MATLAB.

Choosing the Smoothing Parameter

For both methods of detecting the activation time, we optimized our smoothing spline. The smoothing spline, *f,* minimizes the following function:

$$p\sum_{j=1}^{n}\left|y(:,j)-f(x(j))\right|^2+(1-p)\int\left|D^2f(t)\right|^2\,dt \tag{2}$$

where ***x(j)*** is the time at the **j**th time point, ***n*** is the number of data points, ***p*** is the smoothing parameter, ***y*** is the data value, ***D^{2}f(t)*** is the second derivative of the smoothing fit function.

The smoothing parameter can be chosen between 0 and 1. For lower values, the fit over-smoothes and approaches a linear fit, which does not contain information about the activation time. For higher values, p~1, the fit just connects all the data points and is too sensitive to small experimental errors. This leads to inconsistent results among experimental replicates. Therefore, we can test the smoothing parameters by comparing the standard deviations for the distributions of the activation times from a set of experimental replicates.

To identify the best method and its associated optimal smoothing parameter, we produced a set of training data, which is composed of time series containing a step-wise change in transcription rate, ***r***, at time ***t_0*** and a small initial mRNA concentration, ***X_0***. The analytical solution to equation 1 is as follows:

$$\frac{dX}{dt}=\begin{cases}-\lambda X, & for\ t<t_0\\ r-\lambda X, & for\ t\geq t_0\end{cases} \tag{3}$$

$$X=X_0\ \ at\ \ t=0 \tag{4}$$

$$X(t)=\begin{cases}X_0\,e^{-\lambda t}, & t<t_0\\ \frac{r}{\lambda}+\left(X_0-\frac{re^{\lambda t_0}}{\lambda}\right)e^{-\lambda t}, & t\geq t_0\end{cases} \tag{5}$$

When we introduce a uniformly distributed noise function $\rho(t)$, multiplied by a tunable noise coefficient η, the expression profile becomes:

$$X(t) = \begin{cases} X_0\, e^{-\lambda t} + \eta\rho(t), & t < t_0 \\ \frac{r}{\lambda} + \left(X_0 - \frac{r e^{\lambda t_0}}{\lambda}\right) e^{-\lambda t} + \eta\rho(t), & t \geq t_0 \end{cases} \quad (6)$$

Good activation time detection will yield little variation in activation times around t_0 in spite of the noise. Therefore, we tested the 1st and the 2nd derivative methods for a range of smoothing parameters (spanning between 0.001 and 0.87) and noise coefficients (from 0.05 to 5) (Figure S1B).
We set the activation time for the simulated data to t_0=13 min. with an initial transcript level X_0 = 1 (a.u.), and tested the training data for a range of noise levels (η is between 0.05 and 5). The mean activation time of the 1st derivative method converged to the correct activation time (±1min) for the smoothing parameter values greater than 0.2 with a slowly increasing variance of ~5 min (Figure S1C). However, the mean activation time for the 2nd derivative method hits the defined activation time 13 min only for smoothing parameter values between 0.001 and 0.03 meanwhile the variation changes from 4 to 8 min and is larger than for the 1st derivative method. For greater smoothing parameters, the 2nd derivative algorithms becomes more unreliable and mean activation time converges to 20 with the variation 9. Therefore, we choose 0.25 as a smoothing parameter and use the 1st derivative method in all our analysis.

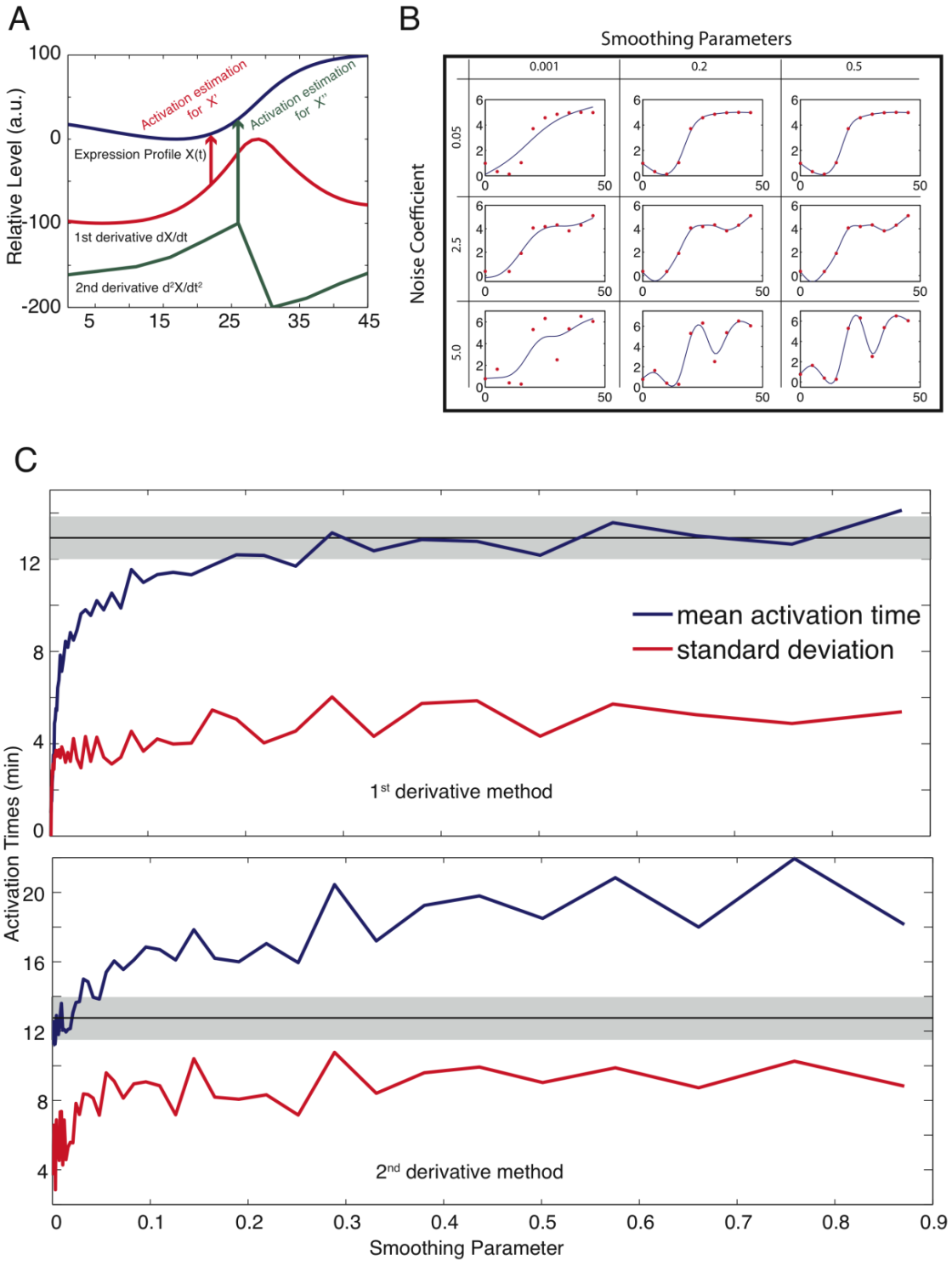
A
Relative Level (a.u.)
100
0
-100
-200
5
15
25
35
45
Activation estimation for X'
Activation estimation for X''
Expression Profile X(t)
1st derivative dX/dt
2nd derivative d²X/dt²
B
Smoothing Parameters
0.001
0.2
0.5
Noise Coefficient
0.05
2.5
5.0
C
mean activation time
standard deviation
1st derivative method
2nd derivative method
Activation Times (min)
Smoothing Parameter

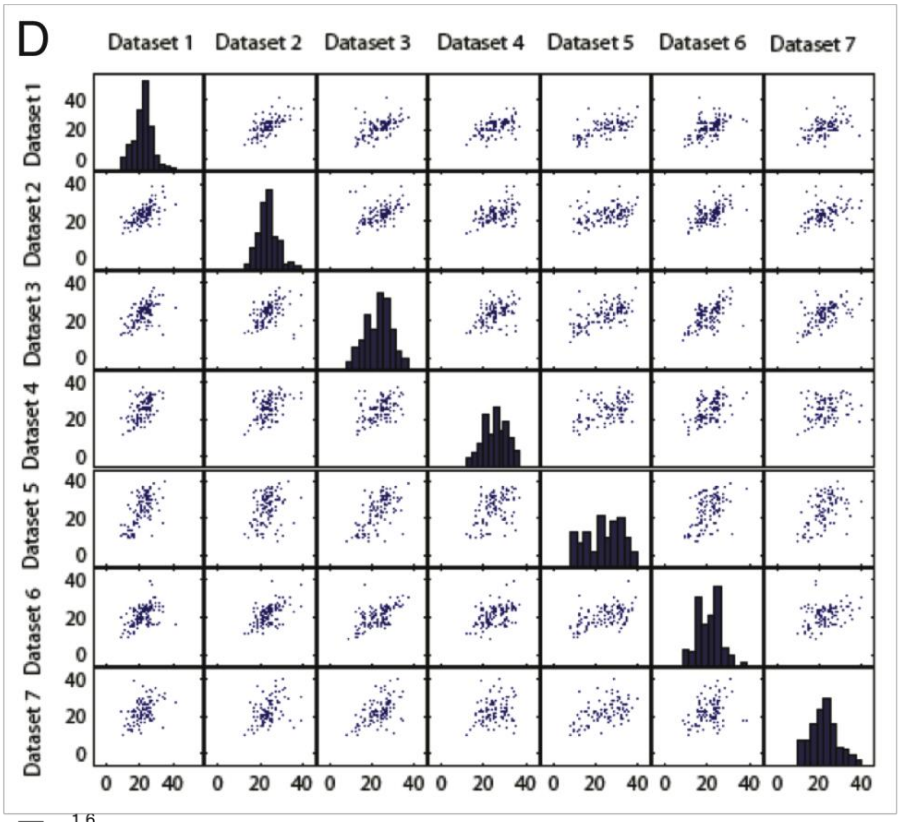
D
Dataset 1
Dataset 2
Dataset 3
Dataset 4
Dataset 5
Dataset 6
Dataset 7

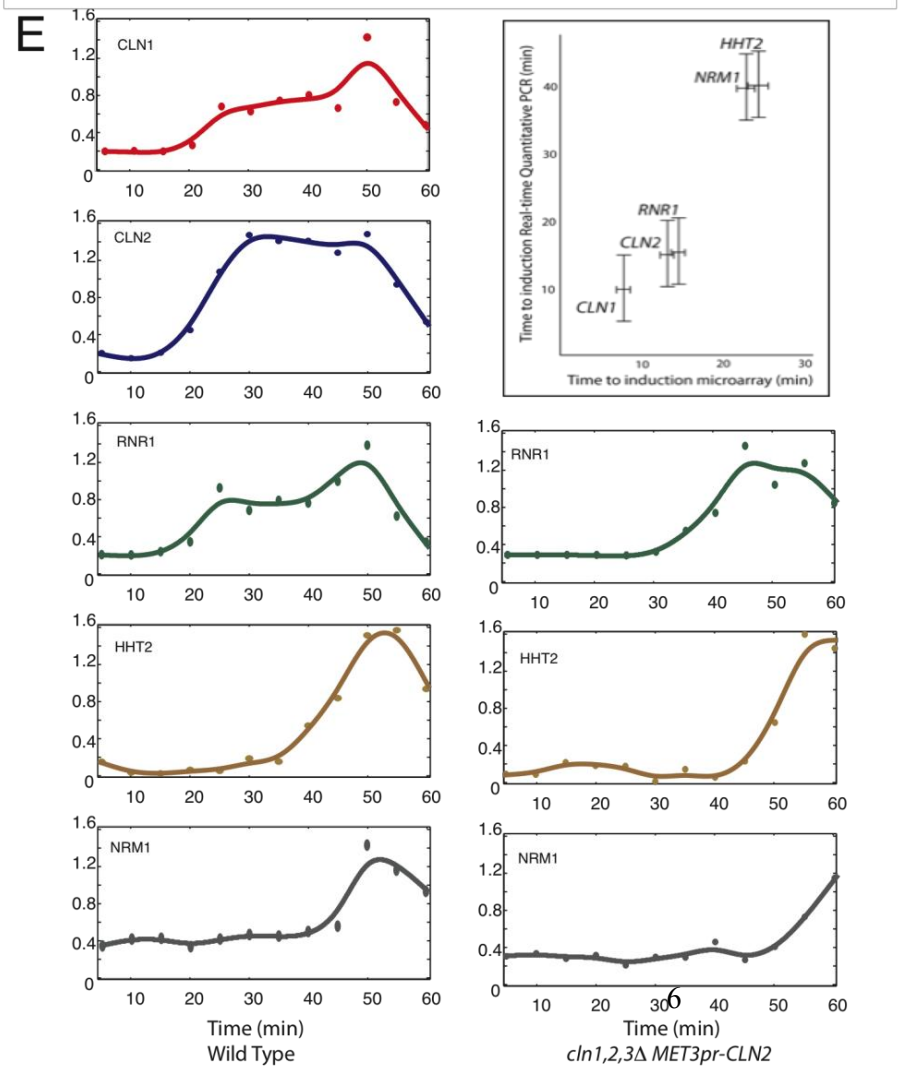
E
CLN1
CLN2
RNR1
HHT2
NRM1
Time to induction Real-time Quantitative PCR (min)
Time to induction microarray (min)
Time (min)
Wild Type
Time (min)
cln1,2,3Δ MET3pr-CLN2

Figure S1. Related to Figure1

A) Activation time of a gene can be calculated using the 1st derivative or the 2nd derivative

B) Simulated data with three different noise levels (red dots) are plotted for three different smoothing parameters. Blue curves show the smoothing spline fit to the data, f(t).

C) The mean (blue) and the standard deviations (red) of the activation times of training set are shown for the 1st derivative method (a), and for the 2nd derivative method (b). We set the activation time to 13 min, shown as the horizontal line. The grey area denotes the activation time t_0 +\- 1min region

D) The scatter plots of each dataset pair is shown in a matrix. Histograms of activation times of each dataset are plotted diagonal. Dataset1: WT, Dataset2: *ash1Δ*,Dataset3: *ace2Δ*, Dataset4: *ash1Δ ace2Δ*, Dataset5: *ASH1**, Dataset6: *ACE2-G128E*, Dataset7: *ASH1* ACE2-G128E*

E) Pheromone and G1-cyclin block-release experiments. Gene expression measured using real time PCR corroborates our conclusions about gene activation timing from microarray analysis. The 3 curves on the RHS are from a cln1Δcln2Δcln3Δ MET3pr-CLN2 G1 block-release time course. Plot in upper RHS corresponds to the pheromone block experiment.

Activation Times of the G1/S Regulon

Table S1. Related to Figure 1

List of genes selected as G1/S regulon

(see the attached spreadsheet file)

Correlation of activation times in 7 mitotic block experiments

We applied our algorithm to the 7 time-course microarray data published by Di Talia et al. (2009). Correlation coefficients, ***R***, are calculated for all pair-wise comparisons by using the following equation:

$$R(X,Y) = \frac{E[(X-\mu_X)(Y-\mu_Y)]}{\sigma_X \sigma_Y}$$

where ***E*** is the expected value operator and μ is the mean value, i.e. μ_X = ***EX***, and σ is the standard deviation. The correlation coefficients are shown in the upper right triangle in the Table S2. The p-values, calculated using kstest, indicate that the activation times of the G1/S regulon members are consistent among all datasets (Table S2).

	Dataset 1	Dataset 2	Dataset 3	Dataset 4	Dataset 5	Dataset 6	Dataset 7
Dataset 1		0.72	0.6	0.59	0.62	0.69	0.56
Dataset 2	2.90E-19		0.72	0.57	0.48	0.59	0.51
Dataset 3	2.30E-11	6.64E-19		0.46	0.55	0.76	0.61
Dataset 4	1.50E-10	1.69E-10	9.62E-07		0.40	0.45	0.21
Dataset 5	5.03E-10	3.77E-06	8.26E-08	4.00E-04		0.57	0.35
Dataset 6	5.89E-16	9.22E-12	1.00E-20	2.13E-06	2.08E-08		0.64
Dataset 7	4.02E-09	5.86E-08	2.78E-11	3.00E-02	1.80E-03	4.62E-12	

Table S2. Related to Figure 1

Correlation coefficients (upper-right triangle, beige) and p-values (lower-left triangle, purple) for all pair-wise comparisons of the distribution of activation times for the 7 mitotic block-release experiments.

Mitotic block release analysis was based on data collected in (Di Talia, Wang et al. 2009). The sequential order of activations is highly consistent between datasets indicating a defined temporal regulation even though the genotypes for the 7 time-courses were not identical (Figure 1F, Figure S1D; Table S2). Di Talia et al (2009) performed the experiment on a set of mutants that in addition to *cdc20Δ GALLpr-CDC20* were otherwise WT, *ash1Δ*, *ace2Δ*, *ash1Δ ace2Δ*, *ASH1**, *ACE2G128E* and *ASH1* ACE2G128E*. *Ace2* and Asch1 are two daughter specific transcription factors, whose mutant versions *ASH1** and *ACE2G128E* are localized to both the daughter and mother cells (Colman-Lerner, Chin et al. 2001; Chartrand, Meng et al. 2002; Laabs, Markwardt et al. 2003). These mutants have been shown to alter *CLN3* mRNA levels, due to the direct regulation of *CLN3* by Ash1 and Ace2 (Di Talia, Wang et al. 2009). Taken together these results suggest that changes in Ash1 and Ace2 distribution and concentration do not affect intra-regulon activation timing and we consider the time-courses as experimental replicates for our analysis.

Cell Size Phenotype in a Late Activated Positive-Feedback System

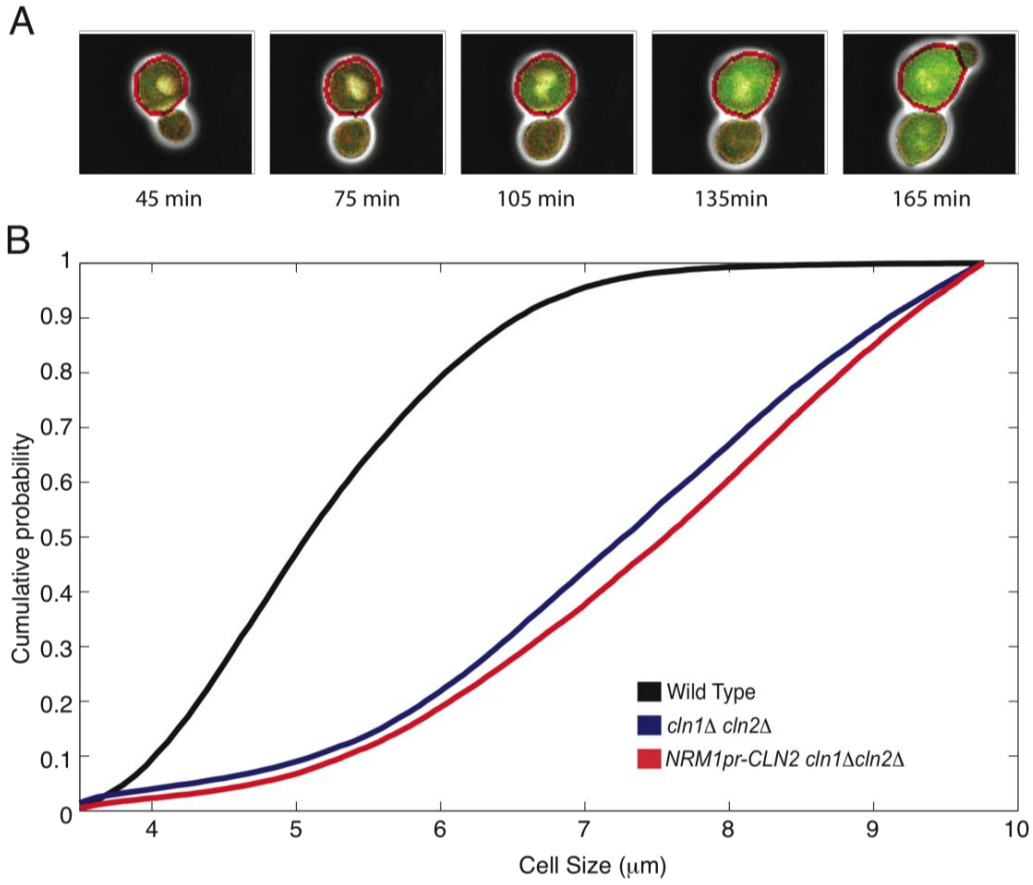

Figure S2. Related to Figure 2

A) Time-lapse microscopy images of the cells having genotype *NRM1pr-CLN2 cln1Δ cln2Δ* are shown. By using an image segmentation program, the cells are automatically detected (red contour). The promoter activations are monitored by fluorescence intensities (GFP for *CLN2* and mCherry for *RAD27*).

B) Delayed positive-feedback cells (*cln1Δ cln2Δ NRM1pr-CLN2*) have a similar cell size phenotype to cln1Δ cln2Δ cells. Cells are grown in log phase and cell size is measured using a Coulter Counter.

Time-Lapse Microscopy Measurements of GFP-Fusion Proteins

Marker	Mean (min)	Standard error (min)	Standard deviation (min)	N
CRH1-GFP	-22.4	1.1	7.6	46
HTB2-GFP	-12.0	0.8	5.1	38
NRM1-GFP	-11.6	1.2	6.8	33
RNR1-GFP	-22.0	2.7	8.1	32
PMT1-GFP	-3.7	0.9	3.8	18
GAS1-GFP	-22.8	1.3	7.0	30
SVS1-GFP	-17.6	1.5	6.4	18
HTA2-GFP	-8.3	0.8	5.8	52
CLN1pr-VenusPEST	-22.5	1.1	7.0	37
CLN2pr-VenusPEST	-23.4	1.1	6.9	20
MNN1-GFP	-12.7	1.6	8.1	25

Table S3. Related to Figures 3 and 4

Activation times (minutes) for protein accumulation are measured relative to bud emergence

Analysis of published microarray datasets

			Distribution of gene activation times			
			G1 block-release		Mitotic block-release	
Data Source	Year	Synchronization	Correlation Coefficient	p-values	Correlation Coefficient	p-values
This work	2010	G1 block	1	0	-0.13	0.15
Di Talia et al.	2009	M block	-0.13	0.15	1	0
Pramila et al.	2006	α factor	0.41	8.44E-11	0.23	0.01
Orlando et al.	2008	Elutriation(WT)	0.48	1.47E-08	-0.02	0.87
Orlando et al.	2008	Elutriation(clbsΔ)	0.65	2.42E-12	-0.17	0.24
Spellman et al	1998	α factor	0.08	0.53	-0.4	0.02
Spellman et al.	1998	cdc15	0.36	4.6E-03	0.04	0.84
Spellman et al.	1998	cdc28	0.26	0.08	-0.39	0.11

Table S4. Related to Figure 4

Comparison of activation time distributions are calculated using previously published datasets *(Spellman, Sherlock et al. 1998; Pramila, Wu et al. 2006; Orlando, Lin et al. 2008; Di Talia, Wang et al. 2009)*

Activation Time of Functional Subgroups

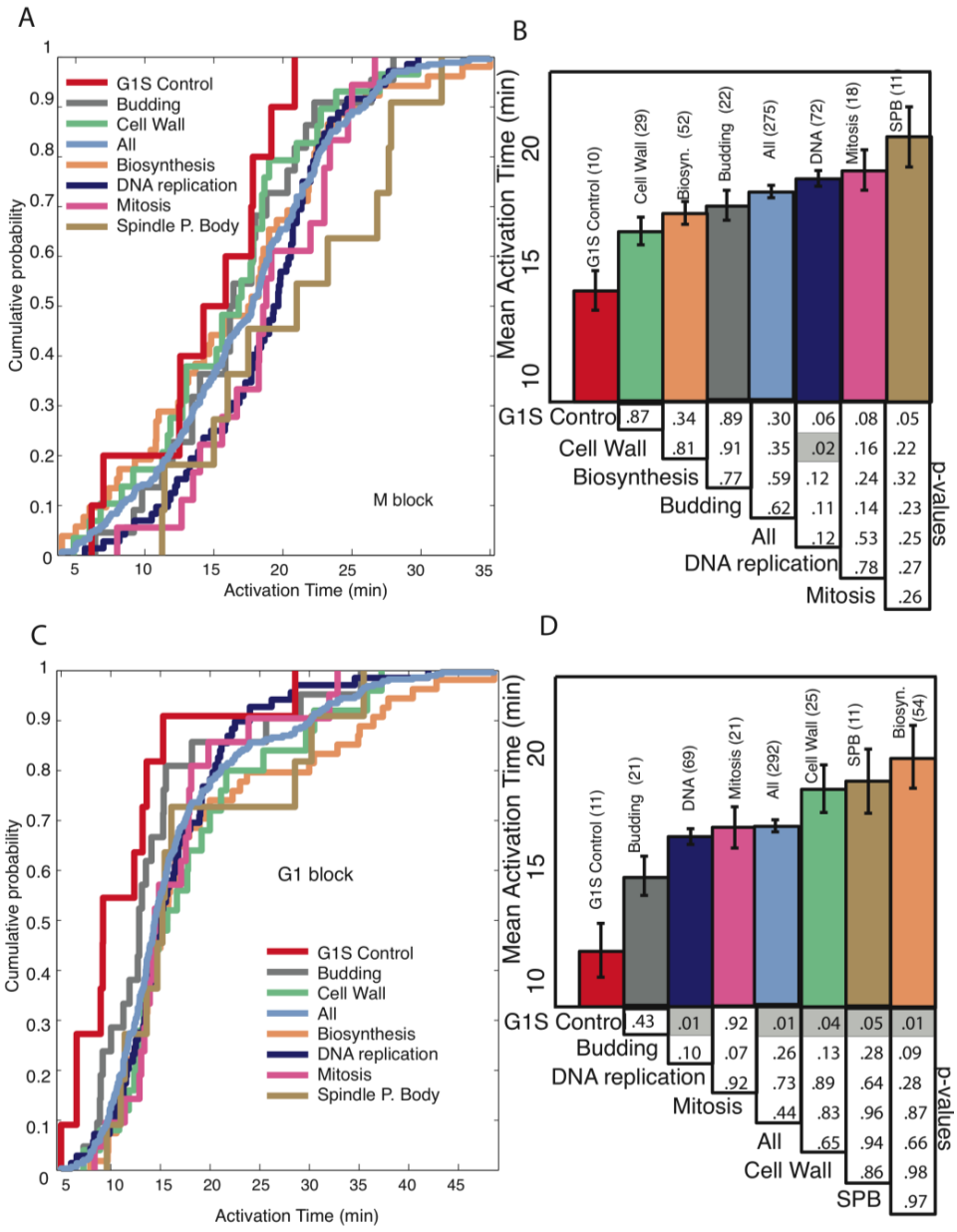

Figure S3. Related to Figure 3

Activation time analysis of functional categories of G1/S regulon in Mitotic and G1 block-release microarray experiments, respectively. Cumulative probability of activation (A),(C) and mean activation time (B),(D) of each functional subgroup with standard error of the mean and the p-values of pair-wise comparisons are shown.

Inactivation Times of SBF and MBF Specific Targets

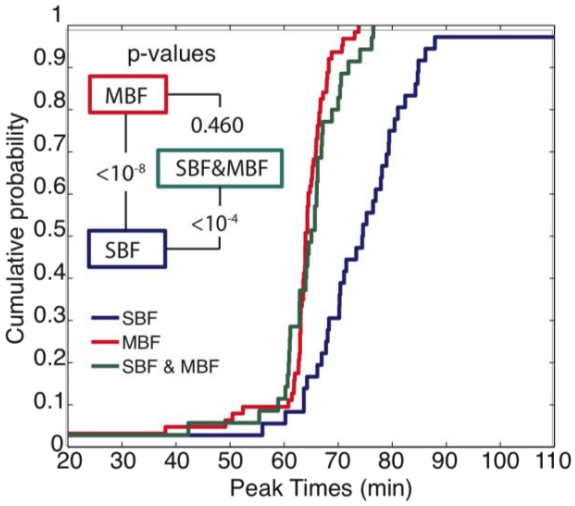

Figure S4. Related to Figure 5

Cumulative distribution of inactivation for SBF-only, MBF-only, and SBF/MBF dual regulated targets. The analyzed microarray data was from Orlando et al (2008). To further investigate the logic of transcriptional inactivation, we analyzed the previously published time-course microarray data where the cells were synchronized via elutriation (Orlando, Lin et al. 2008). We found the result consistent with the analysis in the main text. The SBF and MBF dual regulated targets have the same inactivation time distribution as the MBF-only targets, supporting the Boolean OR-gate model of transcriptional inactivation.

HeLa Microarray Analyses

Table S5. Related to Figure 7
List of E2F target genes analyzed
(see the attached spreadsheet file)

Yeast Strains and Experimental Procedures

Name	Genotype	Source
JS38-1a	*MATa cln1Δ::HIS3 cln2Δ cln3Δ::LEU2 TRP1::MET3pr-CLN2 HTB2-mCherry-spHIS5 WHI5-GFP-kanMX ADE2 ura3-1 can1-1* (W303 background)	(Skotheim, Di Talia et al. 2008)
JS163-8d	*MATa bar1Δ::URA3 ADE2 leu2-3,100 his3-11,15 trp1-1 can1-1* (W303 background)	This study
JS209	*MATa his3Δ1 leu2Δ0 met15Δ0 ura3Δ0 CLN2::CLN2pr-Venus$_{PEST}$* (BY4741 background)	This study
JS210	*MATa his3Δ1 leu2Δ0 met15Δ0 ura3Δ0 CLN1::CLN1pr-Venus$_{PEST}$* (BY4741 background)	This study

C-terminal GFP fusion strains in the BY4741 background used for live-cell imaging were from the UCSF collection (Ghaemmaghami, Huh et al. 2003). We created JS209 by integrating pJS19 at the *CLN2* locus after EcoNI digestion. Similarly, we created JS201 by integrating pJS25 at the *CLN1* locus after AgeI digestion. We created JS218 by digesting pJS50 with EcoNI to integrate the plasmid at the *NRM1* locus.

Plasmids

Name	Description	Source
pJS19	pRS406-*CLN2pr-Venus-PEST*	This study
pJS25	pRS406-*CLN1pr-Venus-PEST*	This study
pGC08D	pRS404-*CLN2pr-Venus-PEST*	G. Charvin

pGC08D was a kind gift from G. Charvin. To construct pJS19, the *CLN2pr-Venus-PEST* insert from pGC08D was ligated to the pRS406 vector following digestion with BglI. A 1kb *CLN1* promoter fragment with terminal PacI and BamHI restriction sites was obtained by PCR of genomic DNA to replace the 1kb *CLN2* promoter in pJS19 to create pJS25.

Supplemental References

Di Talia, S., H. Wang, et al. (2009). "Daughter-specific transcription factors regulate cell size control in budding yeast." PLoS Biol 7(10): e1000221.

Ghaemmaghami, S., W. K. Huh, et al. (2003). "Global analysis of protein expression in yeast." Nature 425(6959): 737-741.

Grigull, J. (2004). "Genome-Wide Analysis of mRNA Stability Using Transcription Inhibitors and Microarrays Reveals Posttranscriptional Control of Ribosome Biogenesis Factors." Molecular and Cellular biology 24(12): 14.

Orlando, D. A., C. Y. Lin, et al. (2008). "Global control of cell-cycle transcription by coupled CDK and network oscillators." Nature 453(7197): 944-947.

Pramila, T., W. Wu, et al. (2006). "The Forkhead transcription factor Hcm1 regulates chromosome segregation genes and fills the S-phase gap in the transcriptional circuitry of the cell cycle." Genes Dev 20(16): 2266-2278.

Skotheim, J. M., S. Di Talia, et al. (2008). "Positive feedback of G1 cyclins ensures coherent cell cycle entry." Nature 454(7202): 291-296.

Spellman, P. T., G. Sherlock, et al. (1998). "Comprehensive identification of cell cycle-regulated genes of the yeast Saccharomyces cerevisiae by microarray hybridization." Mol Biol Cell 9(12): 3273-3297.